January 30, 1966

Final Report | *June 1, 1963 to January 30, 1966*

MECHANICAL PROPERTIES OF CROSSLINKED POLY(METHYL METHACRYLATE) POLYMERS UNDER SPACE ENVIRONMENTAL CONDITIONS

Prepared for:

NATIONAL AERONAUTICS AND SPACE ADMINISTRATION
WASHINGTON 25, D. C.

CONTRACT NASr-49(13)

By: J. E. FREDERICK N. W. TSCHOEGL THOR L. SMITH

SRI Project PRU-4520

Approved: L. A. DICKINSON, DIRECTOR
POLYMER & PROPULSION SCIENCES DIVISION

Copy No. ...6.....

ABSTRACT

Poly-(methylmethacrylate) polymers crosslinked with ethylene glycol dimethacrylate and with hexamethylene glycol dimethacrylate were studied in vacuum (ca. 1 micron) up to about 245°C by the continuous and intermittent stress-relaxation method. At 225°C, the stress remained constant during periods exceeding 1000 minutes even though a 14% weight loss occurred. The stress decayed exponentially at 245°C; the decay constant is inversely proportional to the crosslinker concentration, except at a very low concentration. In all instances, the continuously and intermittently determined stresses were identical and the degradation characteristics were not dependent on the type of crosslinking agent. Degradation under an atmospheric environment was also studied.

Tensile stress-strain data were determined at a series of constant extension rates between about 125 and 185°C (rubbery response region) on crosslinked and uncrosslinked polymers. Because of a relatively tight entanglement network, 1-minute moduli between 135 and 165°C are insensitive to crosslinker concentration (except at high levels) and are essentially identical with that for uncrosslinked PMMA. The time and temperature dependence of the large deformation and ultimate properties are considered, along with the effect of temperature and crosslink density on the nonlinear strain function. The dependence of the failure envelope and of the maximum extensibility on crosslink density is also discussed.

CONTENTS

CONTENTS (Concl'd)

LIST OF ILLUSTRATIONS

ILLUSTRATIONS (Cont'd)

ILLUSTRATIONS (Concl'd)

LIST OF TABLES

I INTRODUCTION

Polymers, because of their diverse and unique characteristics, fulfill a variety of needs in engineering applications and are used, for example, as optical, electrical, thermal-control, adhesive, and structural components. To obtain high reliability and an optimum engineering design, quantitative information is needed on the properties of polymers under the anticipated environmental conditions and on the variation in properties caused by changes in chemical structure or physical state.

This final report describes a study of the effects of elevated temperatures, vacuum conditions, and chemical structure on the mechanical properties of poly-(methylmethacrylate) polymers crosslinked to different extents by two different crosslinking agents. The PMMA polymers, which have a glass temperature in the vicinity of 100°C, were selected for the investigation because related studies were being made at the NASA-Ames Research Center.

The program included studies of stability at elevated temperatures under vacuum and atmospheric environments and of tensile stress-strain properties at temperatures below that at which chemical degradation occurs during a test period. To study stability, the continuous and intermittent stress-relaxation techniques were selected since the resultant data normally show the rates for both rupture and formation of mechanically effective network chains. Tensile stress-strain data were determined at various extension rates and temperatures within the range of rubbery response. These data provide information on: (1) relaxation characteristics as a function of time, temperature, and strain; (2) the inherent form of the nonlinear stress-strain curve; and (3) the time and temperature dependence of the ultimate tensile properties. These characteristics depend on the effective crosslink density, network topology, and the response rate of segments and clusters of chains.

The experimental work was predicated on the assumption that the mechanical properties in the rubbery response region depend primarily

on the effective crosslink density and that the rate of change of crosslink density in a degrading environment can be derived from continuous and intermittent stress-relaxation data. If the mechanical properties depend on crosslink density in a known manner and if the degradation rate in a severe environment at various temperatures is also known, it should be possible to predict--at least semi-quantitatively--the changes in mechanical properties effected by varying environmental conditions.

This report contains a discussion of (1) the PMMA polymers studied and their network topologies; (2) the stability of crosslinked PMMA polymers in vacuum and atmospheric environments; and (3) the large deformation and ultimate tensile properties of several series of PMMA polymers. The Appendices give a discussion of the relaxometer and procedures for procuring data under vacuum conditions, the method for obtaining tensile data, and published literature on properties of PMMA polymers.

II POLY-(METHYLMETHACRYLATE) POLYMERS AND THEIR NETWORK TOPOLOGIES

A. Sample Characteristics, Crosslinker Concentration, and Equilibrium Swelling Experiments

Large sheets of PMMA crosslinked with ethylene glycol dimethacrylate (EDMA) and with hexamethylene glycol dimethacrylate were procured by the NASA Ames Research Center from the Polycast Corporation, Stamford, Connecticut. The weight percent of crosslinker used in the preparation of each polymer is included in Table I which also gives density data obtained at 25°C by the hydrostatic weighing method. A polymer which contains 16% HDMA, designated Lot 12 and not listed in Table I, was also procured. Two uncrosslinked PMMA polymers (designation, Lots 1 and 9) were also prepared by the Polycast Corp.; these materials are sensibly identical and the density of Lot 1 was found to be 1.185 grams/ml. All "Polycast" polymers were prepared using 0.1% α,α'-azobisisobutyronitrile (AIBN) as the polymerization catalyst. All sheets were of excellent physical quality and about 0.040 inch thick. Specimens, when heated above their glass temperature, showed no tendency to warp or curl, indicating an absence of "built-in" stresses.

In addition to those from the Polycast Corp., PMMA polymers crosslinked with 0.3% and 0.8% EDMA were prepared at the Ames Research Center; AIBN was again used as the curing catalyst. These samples contained "built-in" stresses and they became highly distorted when heated above their glass temperatures. The built-in stresses probably resulted from non-uniform polymerization conditions and the shrinkage which accompanies polymerization. Although the thermal stabilities of these samples were not evaluated, their tensile stress-strain properties were studied, as discussed in Section IV.

An estimate of the crosslink density and sol fraction* for each crosslinked PMMA polymer (Polycast) was obtained by determining the

*The sol in a crosslinked polymer is that material which is not connected by primary valence bonds to the network and which thus can be extracted by a suitable solvent.

TABLE I

COMPOSITION AND CHARACTERISTICS OF CROSSLINKED PMMA POLYMERS
(Polycast)

Lot No.	Cross-linker	Weight % Crosslinker	Gel Fraction from Swelling		Mole of Network Chains per ml x 10^4			Density at 25°C, grams/ml
					From Swelling		From Amount of Crosslinker	
			$(CH_2Cl)_2$	$CHCl_3$	$(CH_2Cl)_2$	$CHCl_2$		
17	EDMA	0.04	0.93	0.89	2.08	1.36	0.048	1.188
18	EDMA	0.10	0.92	0.90	1.34	1.53	0.12	1.190
2	EDMA	0.25	0.94	0.83(?)	2.21	1.48	0.30	1.185
3	EDMA	1.0	0.94	0.98	4.54	4.83	1.2	1.185
4	EDMA	6.0	0.94	0.91	9.57	7.59	7.15	--
5	EDMA	16.0	0.96	0.96	33.8	26.1	19.2	--
19	HDMA	0.04	0.92	0.90	0.82	0.83	0.037	1.188
20	HDMA	0.10	0.92	0.90	1.57	1.38	0.093	1.189
10	HDMA	0.25	0.95	0.96	1.85	2.01	0.23	1.185
11	HDMA	1.0	0.90	0.91	3.07	2.59	0.93	1.185
12	HDMA	6.0	0.95	0.95	17.1	13.3	5.55	--

equilibrium swelling in 1,2-dichloroethane and in chloroform. Data were obtained by placing weighted specimens in about 100 ml of 1,2-dichloroethane. Each swollen specimen was weighed perodically until it attained a constant weight; during this time, the solvent was changed several times. This procedure was unsuitable for swelling specimens in chloroform; upon immersing specimens in chloroform, they cracked and tended to fragment. Thus, weighed specimens were placed in refluxing n-butyl acetate at 125°C for about one hour and then allowed to remain for about 5 days in this solvent at ambient temperature. (Specimens of Lot 3 were left in the refluxing solvent for 24 hours.) The swollen specimens were then transferred to chloroform; the solvent was changed periodically and the specimens allowed to swell until they attained a constant weight.

Swollen specimens were dried to constant weight in a vacuum oven at 130-165°C. From the final dry weight and the initial weight, the gel fraction was computed; the results are given in Table I. Values from the tests made with the two solvents are in reasonably good agreement. Roughly speaking, the PMMA polymers contain 10% sol.

The moles of effective network chains per unit volume of initial material was calculated from the equation:[1]

$$(\nu_e)_{sw} = \frac{-[\chi_1 v_2 + v_2 + \ln (1-v_2)]g}{[v_2^{1/3} g^{2/3} - v_2/2]V_1} \qquad (1)$$

where χ_1 is the polymer-solvent interaction parameter, V_1 is the molar volume of solvent, v_2 is the volume fraction of polymer in a swollen specimen, and g is the gel fraction, i.e., (1-g) is the sol fraction. (In this report, the subscript sw added to the symbol ν_e designates results from swelling experiments.) The values[2] used for χ_1 were 0.37 for chloroform and 0.42 for 1,2-dichloroethane. The resulting values of $(\nu_e)_{sw}$ are given in Table I; those for Lots 17, 18, 19, and 20 are probably less reliable than the others because somewhat uncertain values for the dry weights were obtained.

Crosslink density was also calculated from the weight fraction, W_f, of the crosslinking agent in the polymers. Since each crosslinker molecule

should theoretically give two network chains, the appropriate equation is:

$$(\nu_e)_{ch} = \frac{2\rho W_f}{M_A} \qquad (2)$$

where ρ is the sample density and M_A is the molecular weight of the crosslinker (198 for EDMA and 254 for HDMA). The calculated values are included in Table I. (No attempt was made to account for dangling chains.)

B. Modulus and the Entanglement Network

Table II gives values of the 1-minute tensile modulus, F(1), derived (as discussed in Section IV) from stress-strain data obtained at different extension rates and temperatures. One-minute isochronal stress-strain data were used to prepare plots of $\lambda\sigma$ vs. λ-1 and the modulus values were obtained from the initial slopes of these plots. (Typical plots are shown in Fig. 23 in Section IV-C.) Since the F(1) values do not become temperature-independent at elevated temperatures, it appears that equilibrium values were not obtained. For one of the polymers (Lot 2), the slopes of plots* of log σ vs. log t (each curve for a constant λ) showed a greater deviation from zero at 185°C than at 165°C, i.e., the relaxation rate was greater at the higher temperature. (Data at 185°C were analyzed for only three crosslinked polymers.) Although this behavior may reflect the occurrence of chemical degradation during the test periods at 185°C, it may also result from the relaxation (slippage) of entangled network chains, as considered in the subsequent paragraph. However, modulus values** at 165°C are considered to be proportional to the effective crosslink density. This assumption is an expedient one because: (1) the modulus of a lightly crosslinked PMMA sample at 165°C will deviate from the equilibrium value by an amount greater than that for a tightly crosslinked one; and (2) the crosslink density may be more nearly proportional to $2C_1$ in the Mooney-Rivlin equation** than to the equilibrium modulus.

*The 1-minute isochronal stress-strain data were read from these plots.

**A discussion of equilibrium and time-dependent stress-strain data and also of methods for estimating crosslink density are given in the initial portion of Section IV.

Table II

ONE-MINUTE MODULUS DATA FOR PMMA POLYMERS (POLYCAST)
AT TEMPERATURES BETWEEN 125 and 185°C

Cross-linker	Lot No.	F(1),[a] psi				
		125°C	135°C	145°C	165°C	185°C
None	1	--	363	343	269	175
None	9	--	--	355	270	178
EDMA	17	440	362	330	286	--
EDMA	18	460	340	313	287	--
EDMA	2	494	340	327	294	246
EDMA	3	750	454	456	425	408
EDMA	4	--	--	848[b]	725[b]	--
EDMA	5[c]	--	--	--	--	--
HDMA	19	448	353	336	292	--
HDMA	20	455	358	322	288	--
HDMA	10	530	346	322	288	--
HDMA	11	540	365	363	340	320
HDMA	12[d]	--	--	--	--	--

[a] Obtained from slope of plots of $\lambda\sigma$ vs. $\lambda-1$ prepared from 1-minute stress-strain data from tensile tests made at constant extension rates. (Modulus values are not temperature reduced.)

[b] Values not highly precise since they are obtained from data at elongations less than 30%. At higher extensions, specimens either broke or the plot of $\lambda\sigma$ vs. $\lambda-1$ became nonlinear.

[c] Tests were not made on this highly crosslinked material because of its low extensibility.

[d] Stress-strain data not analyzed because specimens broke at small elongations.

(Values of $2C_1$ were derived from the stress-strain data, but these were not sensibly independent of temperature as was found previously[3,4] for a series of Viton A-HV (hydrofluorocarbon) vulcanizates. Thus, it did not seem appropriate to assume that $2C_1$ at a arbitrarily selected temperature is proportional to the crosslink density.) However, if the modulus is in fact more nearly proportional to the crosslink density than is $2C_1$, then the time-dependent modulus (e.g., at 165°C) which reflects the response of both physical entanglements and permanent chains in a network should be used as a characteristic parameter in correlating certain types of data (e.g., maximum extensibility) with network characteristics, whereas the equilibrium modulus should be used in making other types of correlations.

The results in Table II show that the modulus for the two uncrosslinked PMMA polymers (Lots 1 and 9) at 165°C (also at 145 and 135°C) is nearly the same as those for the crosslinked polymers Lots 17, 18, and 2, and Lots 19, 20, and 10. The modulus of uncrosslinked PMMA results from a transient entanglement network; the rather sharp reduction in modulus in passing from 165 to 185°C reflects--at least in large measure--the slippage of entanglements. If such a network also contains chemical (primary valence bond) crosslinks which by themselves give an equilibrium modulus which is considerably less than the modulus for the entanglement network, then the response of the entanglement network will overshadow that of the chemical network and the observed modulus will be that for the entanglement network. This behavior will be observed unless data are obtained at an experimental time which is longer than the time required for relaxation of the entangled chains. For the PMMA samples, this required time may be very long and chemical degradation may begin before entangled chains relax completely.

These considerations point up the difficulty in deciding whether viscoelastic relaxation or chemical degradation is the primary cause for the modulus values being lower at 185 than at 165°C. (It is apparent in retrospect that an answer could probably have been obtained by procuring precise stress-strain-time data in the vacuum relaxometer at temperatures above 165°C.) The considerations of the entanglement network

also explain why the moduli for Lots 17, 18, 2, 19, 20, and 10 are almost identical with that for the uncrosslinked PMMA. Unless the chains in the chemical network have a lower molecular weight than those in the entanglement network, a curve given by a plot of modulus against temperature (or modulus against time) will have either a plateau, or region of slowly changing slope which lies above the equilibrium modulus. In other words, the over-all glass-to-rubber transition contains two dispersions: the second is the transition from the quasi-equilibrium modulus of the entanglement network to the equilibrium modulus. It should be emphasized, however, that the equilibrium modulus is determined by the equilibrium response of chains formed from both chemical crosslinks and permanent entanglement couplings.

Except for several of the most tightly crosslinked PMMA polymers, the data in Table II indicate that the molecular weight of chains between entanglement points is less than that of chains which terminate in chemical junction points. The uncrosslinked PMMA has a 1-minute modulus of 270 psi at 165°C; this formally corresponds to $\nu_e = 1.7 \times 10^{-4}$ mole/ml, or a molecular weight of about 7000. (The molecular weight given by Ferry[5] in his Table 13-II is 8600-10,000, in fair agreement with the present rough estimate.) The value $\nu_e = 1.7 \times 10^{-4}$ is greater than those calculated from the crosslinker concentration (Table I) except for Lots 4, 5, and 12. In conformity with this observation, the modulus of other Lots of PMMA are not markedly greater than that for the uncrosslinked PMMA; however, for Lots 3 and 11, the chemical crosslinks have effected a modest increase (25-60%) in the modulus at 165°C.

C. Equilibrium Swelling, Crosslinker Concentration, and Modulus

The network in a polymer swollen to equilibrium is under a triaxial tensile deformation. During swelling, some entangled chains which contribute to the 1-minute modulus at 165°C will be disentangled; others cannot be disentangled, because of the topological arrangement of chains, and will function as effective chains in the swollen network. Thus, $(\nu_e)_{ch}$ should be related somewhat more closely to $(\nu_e)_{sw}$ than to the

1-minute modulus at 165°C. (The relation may be only slightly better, however.)

This expectation is substantiated by data in Tables I and II which were used to prepare the plot* of log $(\nu_e)_{sw}$ vs. log $(\nu_e)_{ch}$ in Fig. 1.

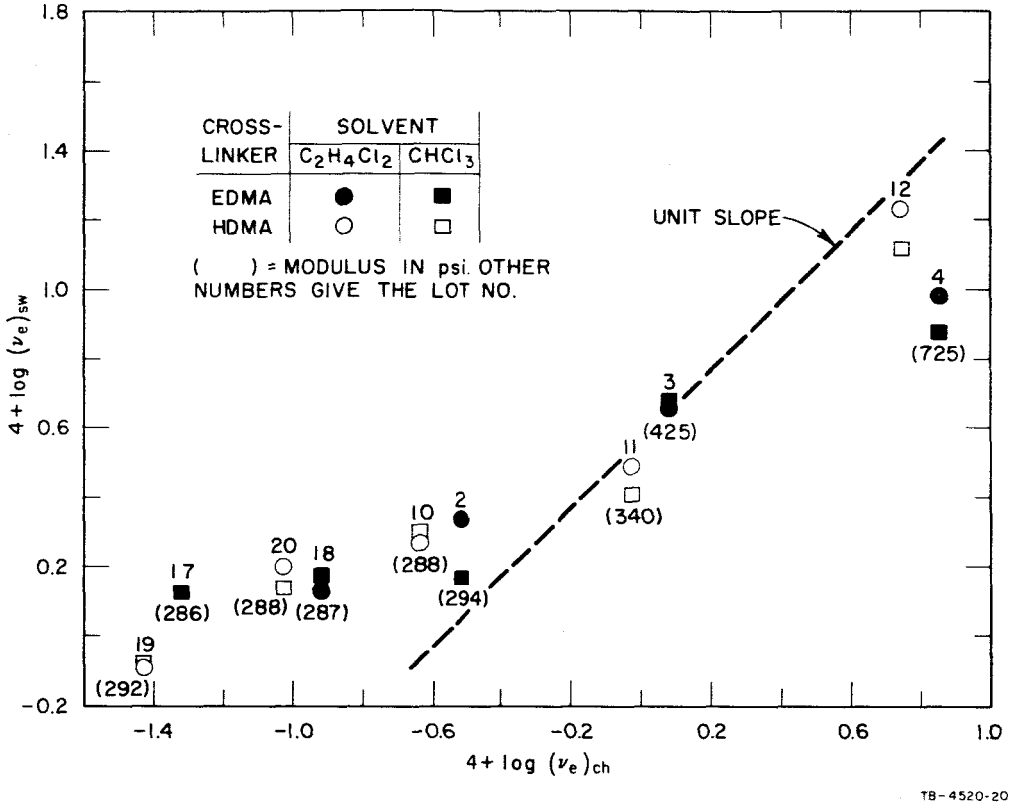

FIG. 1 PLOT OF LOG $(\nu_e)_{sw}$ vs. LOG $(\nu_e)_{ch}$ FOR CROSSLINKED PMMA POLYMERS. (Numbers in parentheses are values of F(1) at 165°C; $(\nu_e)_{ch}$ is from the crosslinker concentration and $(\nu_e)_{sw}$ is from equilibrium swelling data.)

In this figure, the circles and squares represent results from swelling measurements in 1,2-dichloroethane and chloroform, respectively; shaded and open symbols represent the data, respectively, for the EDMA- and HDMA-crosslinked polymers. (The members in the parentheses below the symbols are values of F(1) from Table II.) The dotted line in Fig. 1 shows that a linear relation exists (approximately) between $(\nu_e)_{sw}$ and $(\nu_e)_{ch}$ at the larger values of $(\nu_e)_{ch}$. At the smaller values of $(\nu_e)_{ch}$, $(\nu_e)_{sw}$ is a slowly increasing function of $(\nu_e)_{ch}$.

*The designation $(\nu_e)_{ch}$ is somewhat inappropriate since this quantity is the expected number of chemical chains and not the effective ones.

Figure 2 shows a plot of log $(\nu_e)_{sw}$ vs. log F(1), where F(1) is the 1-minute modulus at 165°C and $(\nu_e)_{sw}$ is here the geometric mean of values

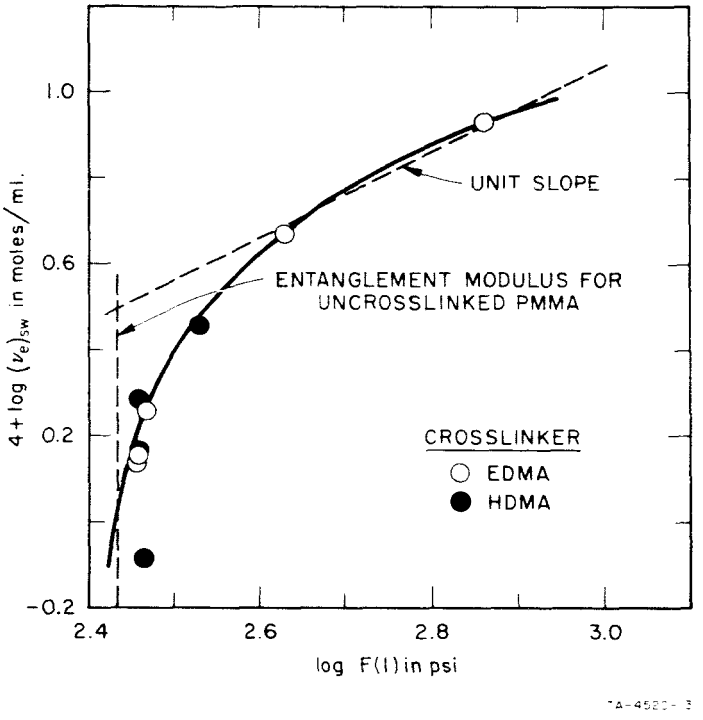

FIG. 2 PLOT OF LOG $(\nu_e)_{sw}$ vs. LOG F(1), WHERE F(1) IS THE 1-MINUTE MODULUS AT 165°C

from swelling in the two solvents. The dotted vertical line is the modulus (entanglement) for uncrosslinked PMMA at 165°C; the dotted line of unit slope shows that a linear relation exists between F(1) and $(\nu_e)_{sw}$ at high crosslink densities. At low crosslinker concentrations, $(\nu_e)_{sw}$ increases about 2.5-fold while F(1) is sensibly constant. This behavior shows that certain chain entanglements which affect F(1) are disrupted during swelling; the number which are disrupted increases with a decrease in the crosslinker concentration.

III DEGRADATION BY CHEMORHEOLOGICAL METHODS

Degradation of PMMA in both atmospheric and vacuum environments was studied by using the continuous and intermittent stress-relaxation technique originated by Tobolsky.[6] The technique consists of measuring the stress on each of two specimens, one of which is extended to the desired strain throughout the experiment and the other is extended to the same strain but only for short intervals during the test (between intervals, the specimen remains in an unstressed state). If the test temperature is above that at which viscoelastic stress-relaxation occurs, the stress on the continuously extended sample is commonly assumed to be proportional to the number of effective network chains. Thus, stress-decay data give a direct measure of the relative number of effective chains broken; any crosslinks which form during degradation will be in their unstrained state and will therefore not contribute to the stress in a continuously extended sample. On the other hand, the stress observed in an intermittently extended sample reflects contributions not only from the network chains originally present but also from newly formed chains. By analyzing the results from continuous and intermittent tests, rate data for both rupture and formation of chains can be derived.

While primary emphasis was placed on determining the stability of the crosslinked PMMA polymers (Polycast) under vacuum conditions, some tests were made under normal atmospheric conditions, as well as in a helium atmosphere, to provide comparative data and supplementary information about polymer characteristics. Several tests were also made on an uncrosslinked PMMA polymer under vacuum conditions.

A. Degradation Under Atmospheric Conditions

An apparatus described elsewhere[7,8] was used for the continuous and intermittent stress-relaxation tests. It contains two load cells mounted on a framework which is immersed in an air thermostat during a test. The apparatus was modified so that tests could be made on ring-shaped specimens, prepared as discussed in Appendix II. The test

procedure was essentially the same as that for the vacuum relaxometer (see Appendix I and Section III-B). One procedural difference is that specimens attained the desired temperature and a test was begun about 30 minutes after the framework and specimens were inserted in the air thermostat; with the vacuum relaxometer, the corresponding period was about 2 hours.

Tests on moderately crosslinked materials, Lots 2 and 3, showed that specimens under strains above about 20% tend to rupture, either immediately upon extension or during a test. Accordingly, a strain of about 10% (near the practical lower limit for stress relaxation) was used in all subsequent tests made with either the vacuum or air relaxometers.

The first tests were made at 200°C but degradation occurred too rapidly to be followed conveniently; all subsequent tests were made at about 182°C. Figure 3 shows the continuous stress-relaxation data for Lot 2 at 185 and 200°C, as well as for Lot 3 at 181°C, on plots of $f(t)/f(0)$ vs. log t, where $f(t)$ is the retractive force at time t, and

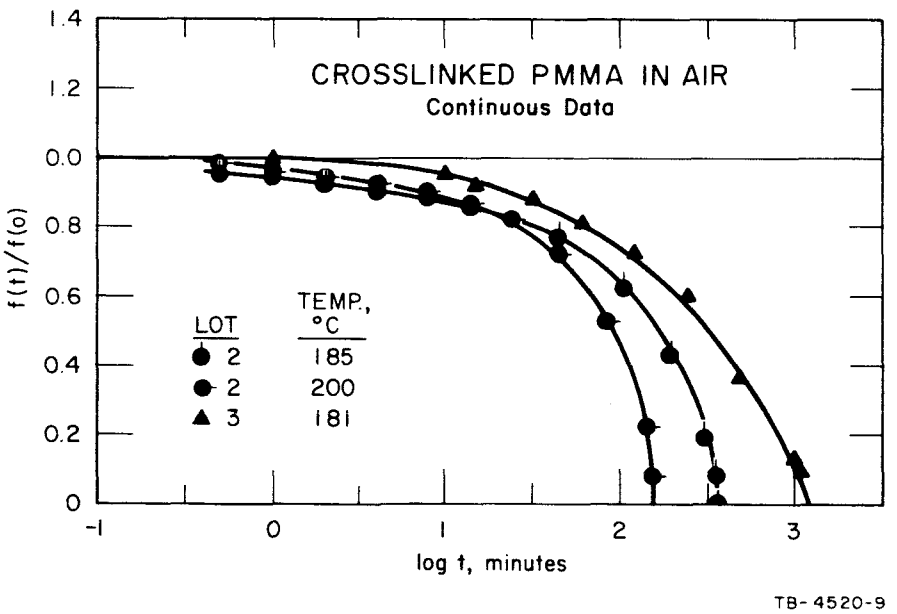

FIG. 3 CONTINUOUS STRESS-RELAXATION DATA ON CROSSLINKED PMMA IN AIR. (Lot 2 at 185 and 200°C and lot 3 at 181°C.)

$f(0)$ is the retractive force at the beginning of the experiment. At 200°C the stress relaxes completely in about 2.5 hours, whereas at the lower temperature about 6 hours is required for complete relaxation.

Both the continuous and intermittent stress-relaxation data, obtained on Lots 2, 3, 10, and 11, were found to be practically identical, as illustrated in Fig. 4 for Lots 3 and 11. This behavior was found regardless of whether EDMA (Lots 2 and 3) or HDMA (Lots 10 and 11) was the crosslinking agent.

The tests showed that the degradation rate does not depend on the type of crosslinking agent. Lots 3 and 11 are crosslinked to comparable degrees with EDMA and HDMA, respectively; the curves in Fig. 4 are essentially identical. Tests on the more lightly crosslinked materials also showed that the relaxation (degradation) rate is independent of the type of crosslinking material.

The effect of crosslink density is shown in Fig. 5, which presents all continuous stress-relaxation data at 182°C. (Since intermittent and continuous data are identical, only the continuous data are shown.) Single lines are drawn through data for samples having similar degrees of crosslinking. The results show that the time required for the force to become zero increases with an increase in the crosslink density.

For most of the curves in Fig. 5, $f(t)/f(0)$ does not equal unity at one minute. Because viscous relaxation occurred when the specimens were first extended and because the degradation began relatively soon, it was not possible to separate the two effects. Consequently, $f(0)$ for the plots was equated to the force observed when a specimen was first extended, and thus $f(0)$ is not an initial equilibrium retractive force.

After all atmospheric tests, evidence of extensive degradation was visually observed; the specimens were slightly discolored, quite friable, and filled with small bubbles. When specimens were not removed immediately from the relaxometer following a test, they often melted into a pile on the lower hook that supports the specimen. These characteristics precluded a determination of the weight decrease which accompanies degradation.

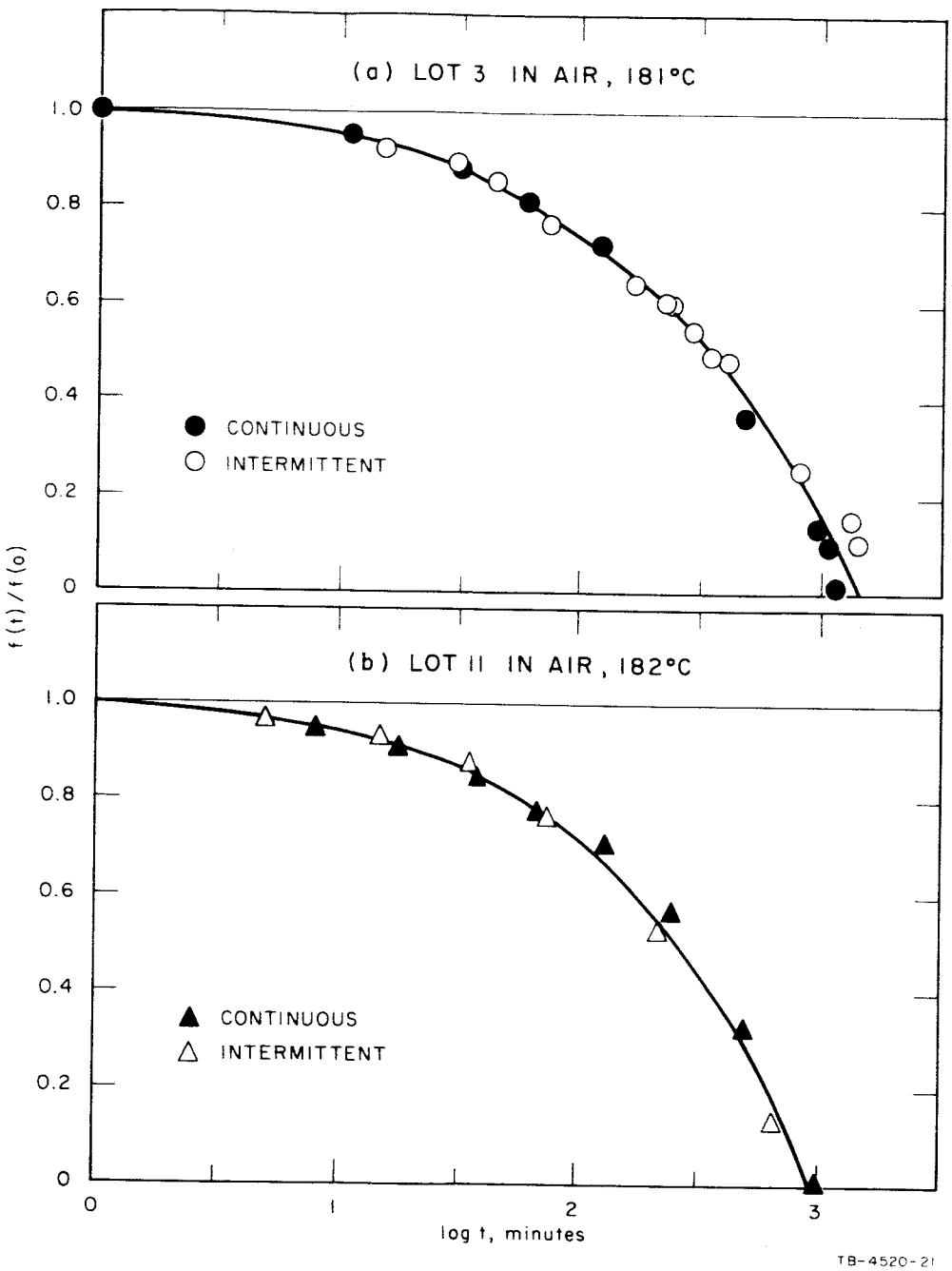

FIG. 4 CONTINUOUS AND INTERMITTENT STRESS-RELAXATION DATA ON CROSSLINKED PMMA IN AIR AT ABOUT 181 °C (Lots 3 and 11)

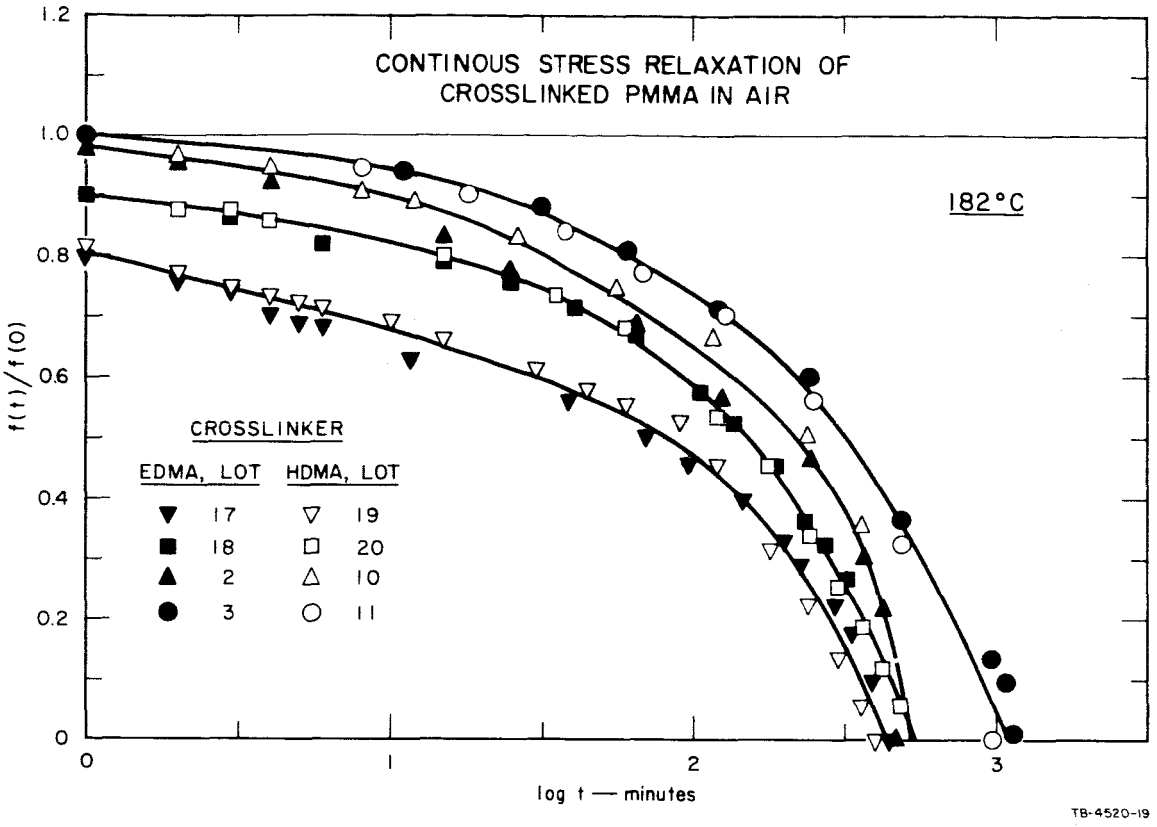

FIG. 5 CONTINUOUS STRESS-RELAXATION DATA ON EIGHT DIFFERENT CROSSLINKED PMMA POLYMERS IN AIR AT 182°C

The atomspheric tests show that the EDMA- and HDMA-crosslinked polymers degrade at the same rate; the rate decreases with an increase in crosslink density and is quite rapid at 180-200°C. The observed identity of the continuous and intermittent data indicates that chains only break during the degradation. Although the results do not preclude the possibility that a few chains may form during degradation, this possibility is an unlikely one. Because bubbles formed in degrading specimens, the data are not sufficiently meaningful to merit a kinetic analysis.

B. Degradation in a Vacuum Environment

1. Apparatus and Experimental Procedures

To study degradation in vacuum at elevated temperatures, a special relaxometer was constructed which allows continuous and intermittent

relaxation data to be obtained simultaneously on specimens under identical environments. (Appendix I gives a detailed description of the apparatus and operational procedures.) In essence, the apparatus contains three load stations mounted beneath a brass plate, through which pass connecting rods for extending the three specimens. Although only two specimens are required for the continuous and intermittent measurements, the third specimen was used in making various preliminary adjustments before a test was begun. The load station assembly is covered by a cylindrical copper housing to form a vacuum chamber.

The vacuum chamber was heated by immersing it in a liquid salt bath which could be thermostatically controlled to $\pm 1^{\circ}C$ at $250^{\circ}C$. Thermocouples embedded within a specimen mounted in the vacuum chamber under less than 1 micron pressure showed that the maximum temperature difference along a specimen was less than $1^{\circ}C$. During all tests, the temperature in the chamber was monitored by several thermocouples, each embedded in a small piece of PMMA, placed in the vicinity of the test specimens. The temperature remained remarkably constant; it varied by less than a few tenths of a degree, although during a test lasting several days, the temperature not uncommonly drifted by one or two degrees.

The vacuum in the chamber, maintained by a mechanical forepump and an oil diffusion pump, was dependent on the outgassing rate of the specimens and thus on the temperature and the characteristics of the material being tested. Test data were obtained at about 1 micron or less.

After specimens were mounted in the chamber, vacuum was applied overnight, and then the chamber was immersed in the liquid bath. Relaxation tests were begun after about two hours--the period required to establish thermal equilibrium in the vacuum chamber. During this heating period, the specimens probably were thoroughly degassed.

Ring-shaped specimens (outside and inside diameters, 1.20 and 1.10 inches, and 0.035-0.045 inch thick) were tested at about 10% extension--a value indicated by the atmospheric tests as likely to be below the rupture strain for specimens of all crosslink densities. The strain was calculated from the inside diameter of the ring at room temperature and the

position of the connecting rod after a specimen was extended. Because it was difficult to account precisely for the thermal expansion of all apparatus components and because of the compliance of the load cells, the strain was not obtained precisely. However, precise strain data were not required since relaxation results are independent of strain, except possibly at very large strains. Specimens were normally weighed before and after tests to determine weight losses which accompany degradation.

2. Relaxation Data for Crosslinked PMMA Samples

Figure 6 shows the continuous and intermittent relaxation data on Lot 3 (EDMA crosslinked) in vacuum at 182, 201, and 224°C and on Lot 11 (HDMA crosslinked) at 223°C. In sharp contrast to results from the atmospheric tests, the stress did not relax in specimens during periods up to 1000 minutes at the elevated temperatures. Data on Lot 11 suggest that some degradation occurred at times greater than 1000 minutes. The slight increase of $f(t)/f(0)$ observed during some tests cannot be real for the continuous data and thus the increase is attributed to recorder drift. The troublesome propensity for the more highly crosslinked samples

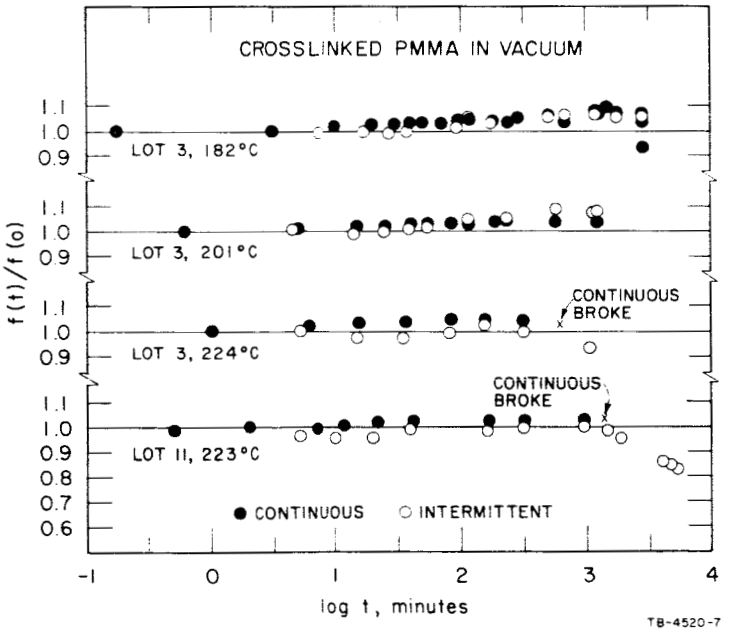

FIG. 6 CONTINUOUS AND INTERMITTENT STRESS-RELAXATION DATA ON CROSSLINKED PMMA IN VACCUM (Lot 3 at 182, 201, and 224°C and Lot 11 at 223°C)

to break during a test (later found to be more pronounced at higher temperatures) is illustrated in Fig. 6 by the continuous data on Lot 3 at 224°C and Lot 11 at 223°C.

The stability in a vacuum environment (about 1 micron) undoubtedly results primarily from the absence of oxygen. To evaluate another environment, a test was made on Lot 2 under 1 atmosphere of helium at 222°C. After installing specimens in the apparatus, the chamber was evacuated at room temperature and then filled with helium; this procedure was repeated three times. The chamber was then immersed in the heated thermostat and the test conducted in the normal manner while maintaining a slight positive pressure of helium. The results in Fig. 7 show that neither the continuous nor intermittent stress changed during a 110-hour period.

Data for comparison with those from the test made under the helium atmosphere were obtained on Lot 2 at 227°C under vacuum conditions. Figure 7 shows that both the continuous and intermittent stress decreased somewhat after about 1000 minutes under vacuum, in contrast to the behavior in the helium atmosphere. It is not known whether this slightly dissimilar behavior results from the vacuum test being made at a 5°C higher temperature than the one in a helium atmosphere or from the oxygen concentration being different during the two tests. It is of interest, however, that during the helium test the weight of the specimen decreased by 7.5%, whereas during the vacuum test it decreased by 27%. This dissimilar behavior may result from the decomposition products being removed more rapidly from a specimen in the vacuum environment.

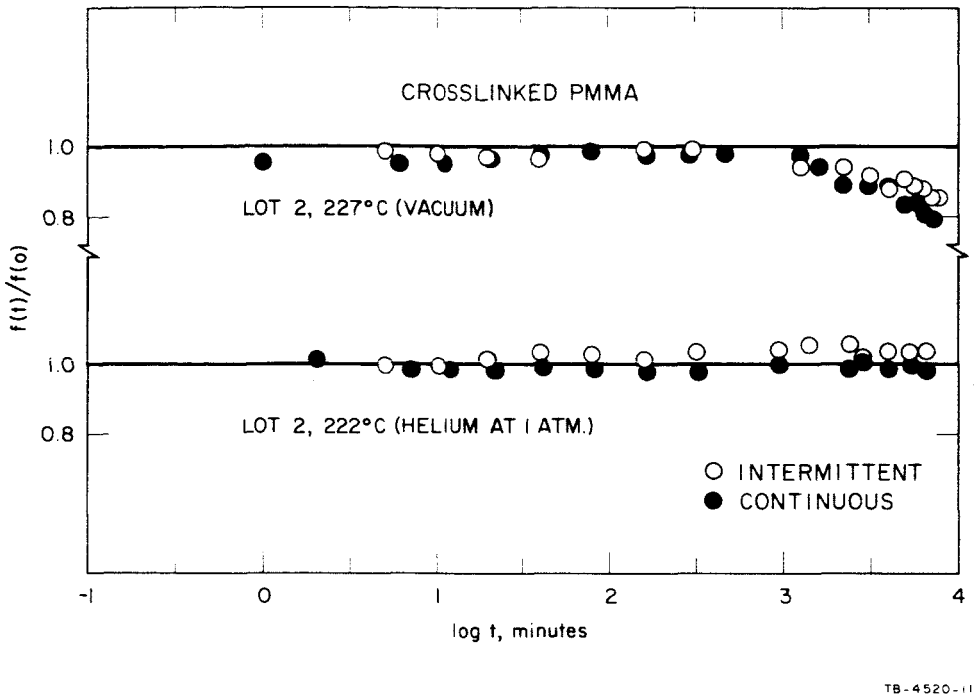

FIG. 7 CONTINUOUS AND INTERMITTENT STRESS-RELAXATION DATA ON CROSSLINKED PMMA (Lot 2) IN VACUUM AT 227°C AND UNDER AN ATMOSPHERE OF HELIUM AT 222°C

Because the stress in the PMMA polymers did not decay significantly during tests at 225°C, tests were made at about 245°C. At this temperature, degradation does indeed occur, as illustrated by data in Fig. 8 on Lots 2 and 10, although the specimens broke before the stress had decreased by a large amount. The results in Fig. 8, as well as those (not shown) on Lots 3 and 11 also at 246°C, show that the continuous and intermittent data are sensibly identical, a characteristic shown by data from atmospheric tests (Section III-A). Figure 9 shows the continuous data at about 245°C for the four EDMA-crosslinked samples, Lots 17, 18, 2, and 3, in order of increasing degree of crosslinking. Data for the corresponding HDMA-crosslinked samples (Lots 19, 20, 10, and 11), shown in Fig. 10, are similar, although not quantitatively superposable with those in Fig. 9.

During the tests at about 245°C, the specimens showed a pronounced tendency to break, even though the strain was only 10%. Specimens from

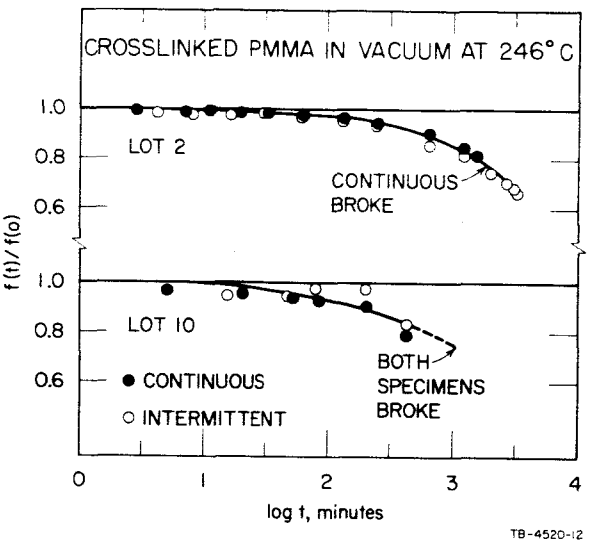

FIG. 8 CONTINUOUS AND INTERMITTENT STRESS-RELAXATION DATA ON CROSSLINKED PMMA IN VACUUM AT 246 °C (Lots 2 and 10)

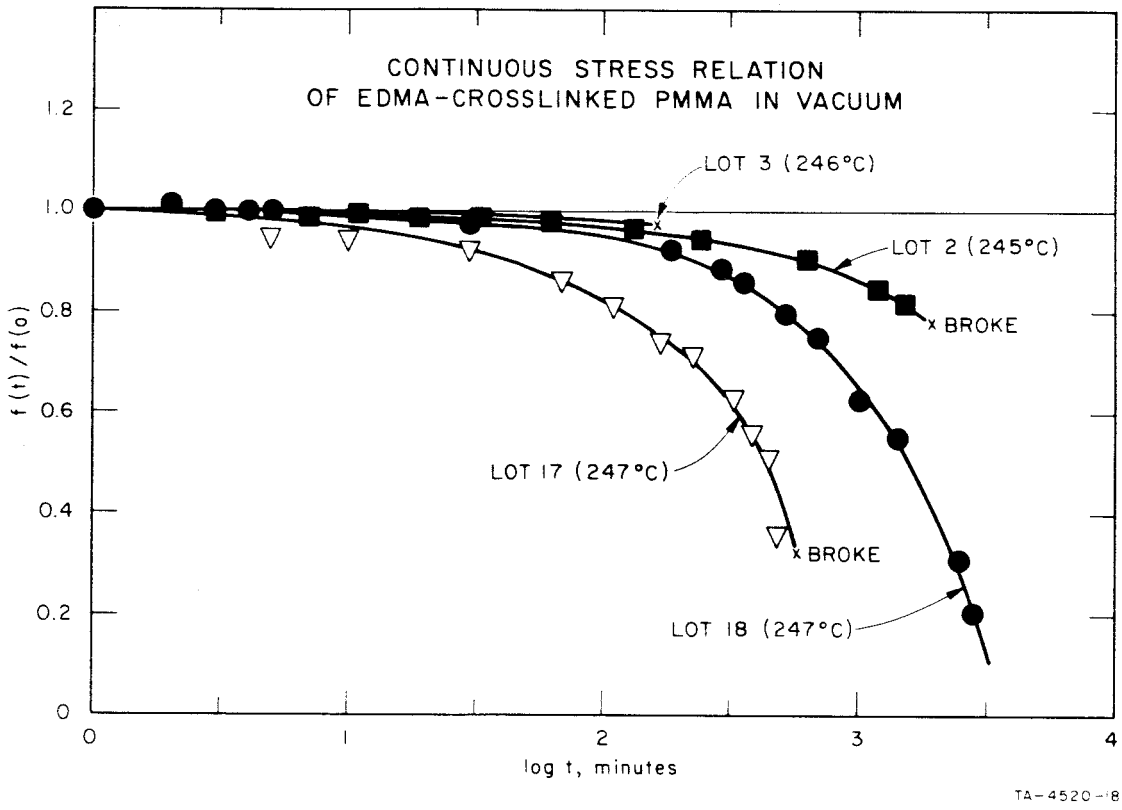

FIG. 9 CONTINUOUS STRESS-RELAXATION DATA ON CROSSLINKED PMMA IN VACUUM AT ABOUT 245°C (EDMA-Crosslinked Polymers, Lots 2, 3, 17, and 18)

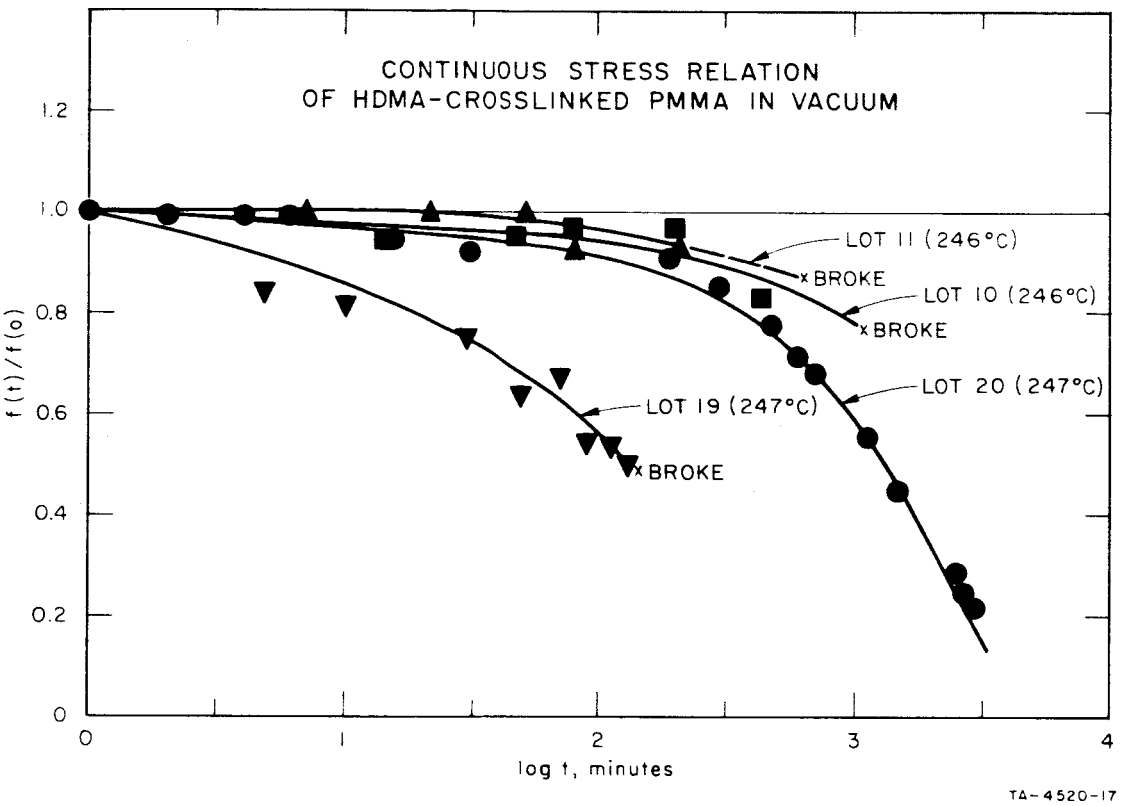

FIG. 10 CONTINUOUS STRESS–RELAXATION DATA ON CROSSLINKED PMMA IN VACUUM AT ABOUT 245°C (HDMA-Crosslinked Polymers, Lots 10, 11, 19, and 20)

Lots 3 and 11 broke soon after the tests began and before degrading appreciably; those from the somewhat less tightly crosslinked Lots 2 and 10 broke after longer periods but still before degrading extensively. However, specimens from the still more lightly crosslinked Lots 18 and 20 did not break, and data were obtained until the stress became almost zero. The most lightly crosslinked polymers, Lots 17 and 19, behaved anomalously in that specimens broke before the tests were completed. However, repeat runs on specimens from Lots 18, 20, 17, and 19 gave the same results as those shown in Figs. 9 and 10. The rupture of the lightly crosslinked Lots 17 and 19 may be related to the large and relatively rapid weight losses which occurred during the tests (Table III). Tests were not made on the most highly crosslinked samples, Lots 4 and 12.

Because of specimen rupture, relaxation data which reflect a major breakdown in network structure were obtained only on Lots 17 and 19 and Lots 18 and 20. At temperatures above 245°C, specimens would unquestionably have broken in a very short period at a 10% strain, and such tests were not attempted.

3. Weight Loss and Degradation Mechanism

In contrast to the highly degraded appearance of specimens after tests in air, the appearance of specimens tested in vacuum at temperatures up to 225°C did not change, in conformity with the finding that the stress did not change during the tests. After tests at 245°C the specimens were slightly discolored, contained a few small bubbles, and their surfaces were not so smooth as initially.

The weight of the specimens decreased (Table III) during tests under vacuum, even when degradation was not indicated by the relaxation data or the visual examination. From thermogravimetric analyses of uncrosslinked PMMA in vacuum, Madorsky[9] found that the weight of a sample whose molecular weight was 1.5×10^4 decreased 43% during 350 minutes at 250°C and 7.4% during 160 minutes at 150°C. For a sample of molecular weight 5.1×10^6, the weight decreased 68% during 315 minutes at 310°C and 0.3% during 160 minutes at 150°C.

Table III

WEIGHT LOSS OF PMMA POLYMERS DURING VACUUM RELAXOMETER TESTS

Run No.	Material	Crosslinker	Temperature, °C	Time, hrs.	Weight Loss, %
38	Lot 17	EDMA	251	15	62.8
39	Lot 18	EDMA	247	59	55.8
43			246	70	62.1
28	Lot 2	EDMA	187	141	15.6
27			222*	113	7.5
25			227	124	26.8
30			245	33	33.4
35			247	45	34.5
24	Lot 3	EDMA	224	18	14.0
33			247	3	14.1
38	Lot 19	HDMA	251	15	57.5
39	Lot 20	HDMA	247	59	56.6
43			246	70	64.0
34	Lot 10	HDMA	246	18	28.5
31			247	32	37
37			244	120	52
26	Lot 11	HDMA	223	88	22.8
32			246	11	20.2
23	Lot 1	None	171	22	4.1
21			182	21	6.7
22			190	21	6.9

*Under helium.

The data in Table III indicate that the extent of volatilization increases with a decrease in the crosslinker concentration and that the EDMA- and HDMA-crosslinked materials behave similarly. The surprising fact is not that the weight decreases, but that the decrease is relatively large during a period in which the stress remains constant. For

example, stress decay did not occur during the 18-hour test on Lot 3 at 224°C but the weight decreased by 14%. When a greater weight loss was observed, the stress decayed during the test.

An appreciable decay in stress was observed only at 245°C, and at this temperature, rupture commonly terminated the tests prematurely. Because rate data were obtained only at 245°C, and only a limited amount at this temperature, the results lead only to tentative conclusions about the kinetics and mechanism of the degradation process.

If chains break randomly throughout a degrading network and if the rate of chain scission is constant, then it can be shown[6] that the force in a specimen held continuously at a constant extension should obey the equation:

$$\frac{f(t)}{f(0)} = \exp(-kt/\nu_e) \qquad (3)$$

where ν_e is the moles of effective network chains per unit volume in the undegraded material and k is the moles of chains per unit volume which break per unit time. Thus, a plot of log $[f(t)/f(0)]$ vs. t should yield a straight line whose slope is $k/2.303\nu_e$.

Data on four PMMA specimens are plotted according to Eq. (3) in Fig. 11; the slopes of the resulting straight lines give the values of k/ν_e which are included in Table IV. When these values are multiplied by $(\nu_e)_{ch}$, computed from the crosslinker concentration, relatively constant values for k are obtained (except for Lot 19) and these are given in the last column of the table. If values of ν_e derived from either modulus data or equilibrium swelling data are used, the resulting values for the rate constant k vary quite markedly. Thus, the rate of stress decay is determined by the number of chemical junction points and is not affected significantly by the entanglement points. Stated otherwise, the decay constant (slope of a plot of $\ln[f(t)/f(0)]$ vs. t) is inversely proportional to the crosslinker concentration.

The thermal degradation of PMMA involves a depolymerization (unzipping) mechanism which yields the monomer almost exclusively.[9a] The

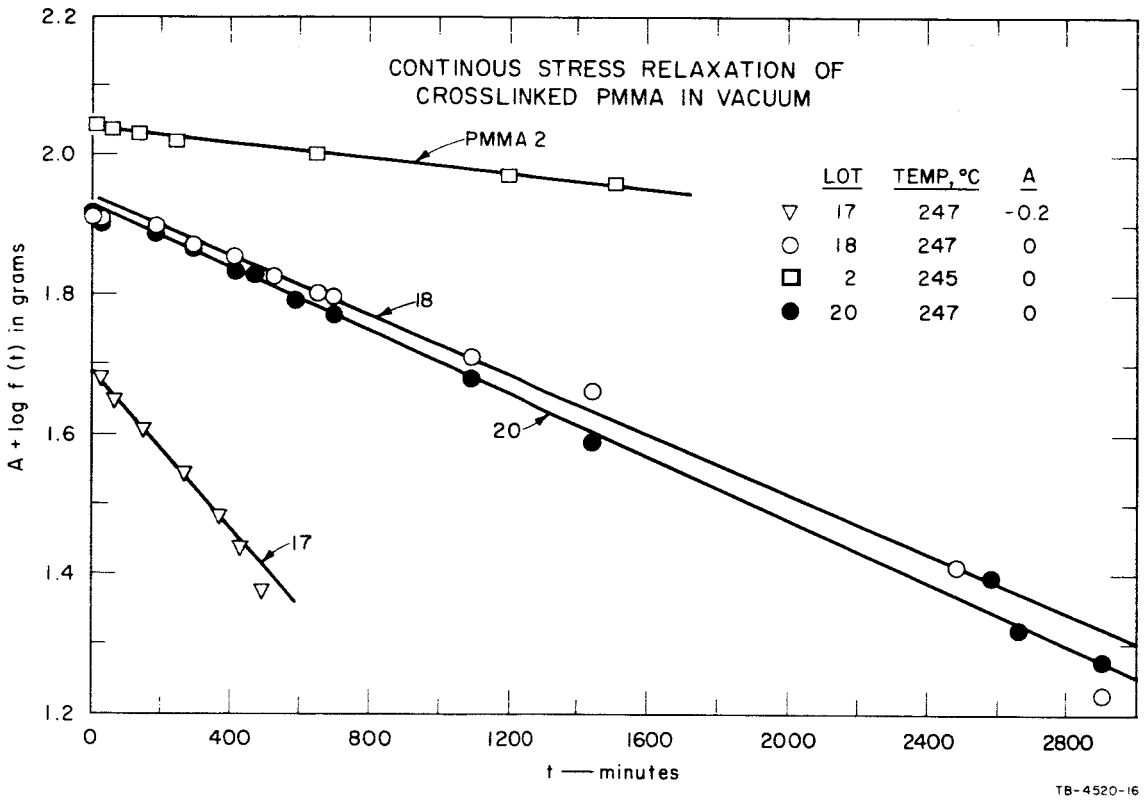

FIG. 11 SEMILOGARITHMIC PLOTS OF FORCE AGAINST TIME FROM CONTINUOUS STRESS-RELAXATION DATA ON CROSSLINKED PMMA (EDMA-Crosslinked Polymers, Lots 2, 17, and 18; HDMA-Crosslinked Polymers, Lot 20)

Table IV

DEGRADATION RATES FOR PMMA POLYMERS IN VACUUM AT ABOUT 245°C

Lot	Temp. °C	$(k/\nu_e)10^4$, min^{-1}	$(\nu_e)_{ch}^{(a)} \times 10^4$ mole/ml	$k \times 10^8$, mole/ml-min
2	245	1.3	0.30	0.39
18	247	4.8	0.12	0.58
20	247	5.3	0.093	0.49
17	247	11	0.048	0.53
19	247	44	0.037	1.6

(a) Obtained from concentration of crosslinker used in preparation of samples (see Table I). If values of ν_e derived from either the tensile modulus or equilibrium swelling data are used, the rate constant k, given in last column, varies markedly.

degradation proceeds from two initiation mechanisms:[9b] the first involves initiation at double bonds, situated at chain ends; the second involves either a random initiation or initiation at chain ends without double bonds. (Certain chain ends contain tertiary hydrogen.) The first type of initiation is responsible for the degradation which proceeds at intermediate temperatures (ca. 200 to 270°C) and which ceases before the entire specimen has decomposed. For one PMMA at temperatures between 240 and 270°C, Madorsky[9] found that the volatilization rate progressively decreases and becomes zero after 40-45% of the original material has volatilized. The second type of initiation becomes important only at quite high temperatures.[9b]

The constancy of k (Table IV) indicates that the chains rupture at a rate which is independent of the chain length between chemical junction points. Yet, the weight loss during a test depends quite strongly on the crosslinker concentration which is inversely related to the chain length. These dissimilar observations are consistent with the assumption

that chain rupture (initiation of decomposition) is followed by a depolymerization of the entire chain between its chemical junction points. Thus, the weight loss would depend on the chain length.

It seems quite unlikely, however, that a depolymerization reaction would be terminated by the presence of a dimethacrylate moiety in a network structure. Also, Grassie and Melville[9c] have studied the decomposition of several crosslinked PMMA polymers and have found that the initial decomposition rate is independent of crosslinker concentration. As yet, a satisfactory explanation has not been found for the present findings, although an analysis of possible mechanisms has not been made. Two points which need detailed examination will be mentioned. The first is the fact that one depolymerizing chain will release a number of entangled chains which contribute to the support of stress in a deformed specimen. The second is that one initiation will decompose, on the average, a chain whose molecular weight is about 200,000. It is of possible significance that for Lot 19 the calculated molecular weight of chains which terminate in a dimethacrylate moiety is about 320,000; this fact may have some relation to the anomalous result derived from the relaxation data. Also, a large amount of the initial weight loss quite likely comes from decomposition of sol material; the concentration of double bonds, at which depolymerization begins, should be markedly greater in the sol than in the network material.

4. Results on Uncrosslinked PMMA

Because the crosslinked PMMA samples show no degradative stress relaxation during a prolonged period under vacuum conditions at 224°C, uncrosslinked PMMA would be expected to be chemically stable at elevated temperatures and stress relaxation should result only from viscous relaxation.

Data from vacuum tests on uncrosslinked PMMA (Lot 1 from Polycast Corp.) at 171, 182, and 190°C are shown in Fig. 12. The continuous stress-relaxation data conform to the expected behavior; on plots of log σ vs. log t, where σ and t are the stress and time, respectively, the curves can be superposed rather well by shifting them along the abscissa.

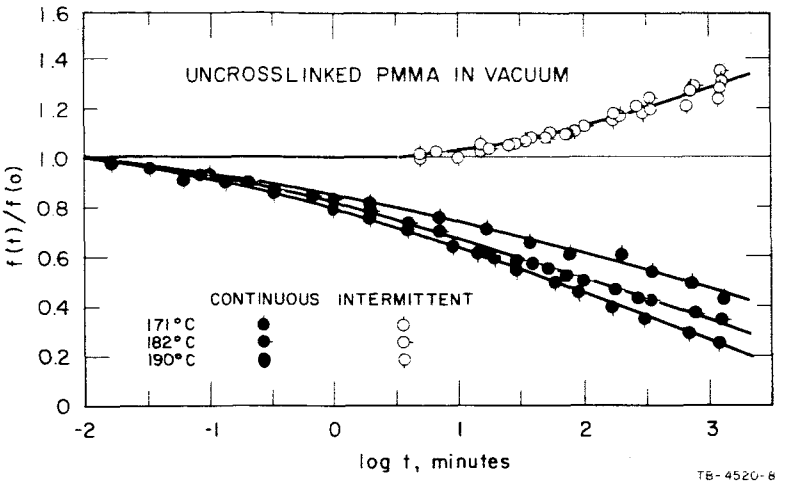

FIG. 12 CONTINUOUS AND INTERMITTENT STRESS-RELAXATION DATA ON UNCROSSLINKED PMMA IN VACUUM AT 171, 182, AND 190°C

The stress measured intermittently increased quite appreciably during the tests at each temperature. The results were carefully checked to determine whether they might be attributed to some malfunction of the relaxometer. No malfunction was found, and the results have been tentatively accepted, especially since they agree qualitatively with the behavior to be expected if low molecular weight chains either volatilize or decompose and then volatilize under the vacuum environmental conditions.

At the test temperatures, the stress determined intermittently should correspond to a point slightly to the right of the plateau on a plot of log σ vs. log t. The width of this plateau becomes greater and extends to a longer time with an increase in molecular weight. During the initial stages of thermal decomposition, the low molecular weight material decomposes preferentially because of its high concentration of double bonds at which decomposition begins. (Grassie[9a] has presented data on PMMA polymers which show that the average molecular weight of the residual material increases during the initial stage of decomposition.) Volatilization of either residual monomer or low molecular weight chains also increases the average molecular weight. During the time required to extend a specimen and determine the stress, less relaxation will occur if the molecular weight is higher and the plateau is broader. Thus, the intermittently observed stress will continuously increase with time because of the gradual widening of the plateau.

IV TENSILE PROPERTIES IN THE ABSENCE OF DEGRADATION

According to the statistical theory of rubberlike elasticity,[10] equilibrium stress-deformation data in uniaxial tension or compression should conform to the equation:

$$\sigma = \nu RT(\lambda - \frac{1}{\lambda^2}) \tag{4}$$

where σ is the stress, based on the cross-sectional area of the undeformed specimen; λ is the extension (stretch) ratio which equals $\epsilon + 1$, ϵ being the Cauchy measure of strain; ν is the moles of network chains per unit volume; and RT is the product of the gas constant and the absolute temperature. Also, according to the theory, $G = \nu RT$, where G is the shear modulus. Because real networks contain inactive chains (those attached to the network at one end only, and those which form small closed loops which do not participate directly in supporting the load on a deformed specimen) and also active chains formed by permanent physical entanglements in the network, ν in Eq. (4) is usually replaced arbitrarily by ν_e, the moles of effective network chains per unit volume.

Equation (4) is based on several assumptions, one of which is that the entropy change which accompanies the deformation of a single chain is related to a Gaussian probability function. This assumption is reasonably valid as long as the end-to-end separation of a chain does not exceed some fraction (say, 0.4) of its fully extended length. To account for behavior at large extensions at which the so-called finite extensibility effects must be considered, several approaches have been followed. One approach[10] leads to an expression for the entropy of a single chain; when applied in an idealized (and somewhat over-simplified) manner to a network, this expression gives an equation, which for uniaxial tension, reduces[11] to:

$$\sigma = \nu RT\left[\frac{n^{\frac{1}{2}}}{3}\,\mathcal{L}^{-1}(\lambda/n^{\frac{1}{2}}) - \frac{1}{\lambda^2}\right] \tag{5}$$

where $\mathcal{L}^{-1}(\lambda/n^{\frac{1}{2}})$ is the inverse Langevin function of the argument $\lambda/n^{\frac{1}{2}}$, and $n^{\frac{1}{2}}$ is related to the maximum extensibility, $(\lambda_\infty)_{max}$, of the network

through the defining relation[11] $n^{\frac{1}{2}} \equiv (\lambda_\infty)_{max}$. Since $\mathcal{L}^{-1}(\lambda/n^{\frac{1}{2}})$ tends toward infinity as λ approaches $n^{\frac{1}{2}}$, the stress becomes infinite at $\lambda = (\lambda_\infty)_{max}$. In the derivation[10] of Eq. (5), n is assumed to be the number of equivalent random links in a chain. Thus, for a series of perfect networks (those devoid of inactive chains and sol material) which have different crosslink densities, the product $n\nu$ is a constant. Consequently, the maximum extensibility should depend on crosslink density according to the equation $(\lambda_\infty)_{max} = K\nu^{-\frac{1}{2}}$, where K is the constant $n\nu$.

If equilibrium data conform to Eq. (4), then ν_e can be evaluated directly. However, uniaxial tensile data usually do not fit Eq. (4), and the data are commonly considered in terms of the Mooney-Rivlin equation:[10,12]

$$\sigma = 2C_1(\lambda - \frac{1}{\lambda^2}) + 2C_2(1 - \frac{1}{\lambda^3}) \qquad (6)$$

where C_1 and C_2 are constants. Data over limited ranges of λ can usually be represented by this equation. Certain results suggest[12] that:

$$2C_1 = \nu_e RT \qquad (7)$$

However, it is unlikely that Eq. (7) applies to all rubbery network polymers, and an unambiguous method for determining ν_e does not exist.

Although equilibrium swelling data are commonly used to evaluate ν_e (e.g., see Section II), the results may be less reliable than those obtained by applying either Eq. (4) or (7). The equation used to relate ν_e to equilibrium swelling data is based on the assumption that the stored elastic energy is given by the same expression which leads to Eq. (4). In addition, the equation contains a semi-empirical polymer-solvent interaction parameter χ_1 which is assumed to be independent of

the polymer concentration in a swollen specimen. The assumption that χ_1 is concentration-independent is commonly an invalid one.

For certain purposes, it is desirable to know the number of backbone atoms in an active network chain and thus the contour length of the chain. The number of backbone atoms is related directly to the molecular weight of the chain, M_c. If ν_e is known, then M_c can be obtained from the equation

$$M_c = \frac{W_c}{\nu_e} \tag{8}$$

where W_c is the weight of active chains in a unit volume of polymer. If a polymer contains neither sol nor inactive chains, then $W_c = \rho$, where ρ is the density of the polymer. Since networks usually contain sol and inactive chains, W_c can be estimated only semi-quantitatively. Also, networks contain a distribution of chain lengths, and even crude methods do not exist for estimating this distribution.

Thus far this discussion has been limited to considerations of equilibrium stress-strain data. However, experimental data are commonly time-dependent and reflect both the relaxation processes which occur during the test period and the inherent stress-strain characteristics of the network. Such time-dependent data can be considered[13] in terms of the equation:

$$\sigma(\lambda,t) = F(t)\Gamma(\lambda) \equiv F(t)\,\frac{(\lambda-1)}{g(\lambda)} \tag{9}$$

where the stress $\sigma(\lambda,t)$ is a function of λ and the time t, $\Gamma(\lambda)$ is a function of λ, and $F(t)$ is the time-dependent modulus defined by:

$$\lim_{\lambda \to 1} \frac{\sigma(\lambda,t)}{\Gamma(\lambda)} = \frac{\sigma(\lambda,t)}{\lambda-1} = F(t) \tag{10}$$

The modulus characterizes the time-dependent behavior under an infinitesimal deformation and it depends on the stress-strain history. However, in conformity with the previously introduced notation,[13] $F(t)$ will be considered here to represent the response to a strain which increases at a constant rate.

Equation (9) is applicable for representing data when $\Gamma(\lambda) \equiv \sigma(\lambda,t)/F(t)$ is time-independent. Data obtained[11,13,14] on many rubber vulcanizates within certain ranges of time and temperature show this characteristic. In such instances, a plot of $\sigma(\lambda,t)/F(t)$ vs. λ yields[11,14] a curve which is identical to that from equilibrium data. At best, however, $\Gamma(\lambda)$ is time-independent only under those experimental conditions for which the terminal (maximum) relaxation time of a single network chain is less than the experimental time-scale. When the experimental time-scale is shorter than the terminal relaxation time, relaxation modes within a chain become effective, causing a reduction in the extensibility of the network. The reduced extensibility causes[14] $\Gamma(\lambda)$ to increase more rapidly--especially at large extensions--and to tend toward infinity at a smaller extension than when the time-scale is long; such phenomenon cause $\Gamma(\lambda)$ to be time-dependent.

For certain rubber vulcanizates, $\Gamma(\lambda)$ is time-dependent even when the experimental time-scale is greater than the terminal relaxation time. The associated molecular processes which lead to the occurrence of relaxation under such conditions--regardless of whether $\Gamma(\lambda)$ is time-dependent or time-independent--are not definitely known. However, the relaxation may result from cooperative chain rearrangements which are associated with either the slippage[15,16] of entangled chains or the migration[17,18] of network junction points.

The stress-at-break, σ_b, and the corresponding ultimate extension ratio, λ_b, depend markedly on the temperature and the extension rate. For amorphous elastomers, data over extended ranges of temperature and extension rate yield a single curve, called the tensile failure envelope,[19,11] on a plot of log $\sigma_b(T_0/T)$ vs. log (λ_b-1), where T and T_0 are, respectively, the test temperature and an arbitrarily selected reference temperature, both expressed in °K. This curve passes through a maximum at $(\lambda_b)_{max}$ which is the maximum observable extension ratio. As discussed,[11] $(\lambda_b)_{max} \leq (\lambda_\infty)_{max}$. For some elastomers, it appears[11] that the equality is sensibly true whereas for others, $(\lambda_b)_{max}$ is significantly less than $(\lambda_\infty)_{max}$. When the latter situation exists, $(\lambda_\infty)_{max}$ is the maximum extension ratio (hypothetical) which could be observed if the network were infinitely strong.

Relatively little is now known about the dependence of $(\lambda_b)_{max}$ on crosslink density and other structural characteristics, but some findings are presented in Ref. 11.

The crosslinked PMMA polymers (Polycast) were tested at various extension rates and temperatures. The two crosslinked samples (Section II-A) prepared at the Ames Research Center were also tested, as well as a commercially available uncrosslinked PMMA material. The results from these tests are presented in the remaining portion of this section, and considered in relation to background information given above and in Sections II-B and II-C. (The method for procuring the data is discussed in Appendix II.)

A. Uncrosslinked PMMA

A commercially available PMMA polymer was tested in the rubbery response regions at eight temperatures between 110 and 165°C and at crossheat speeds between 0.02 and 20 inches per minute. The methods for reducing and analyzing the data differed only in minor details from those developed for other amorphous elastomers.[13] From stress-strain curves at different extension rates, values of stress are obtained at a series of fixed values of λ. Then, the stress data at each λ are displayed on a plot of log σ vs. log t, where the time t equals $(\lambda-1)/\dot{\lambda}$, $\dot{\lambda}$ being the extension (strain) rate.

In analyzing data on PMMA, the temperature-reduced stress $273\sigma/T$ was first plotted against time on a doubly logarithmic plot for several extension ratios at each test temperature. Values of the shift factor a_T were then obtained by shifting the curves to coincidence along the time axis. The resulting shift factors are shown in Fig. 13 in which the solid line represents the universal form of the WLF equation[5]

$$\log a_T = - \frac{8.86(T - T_s)}{101.6 + T - T_s} \qquad (11)$$

This equation gives a_T as a function of $(T-T_s)$, where the characteristic temperature T_s is generally about 50 degrees higher than T_g. Conversely,

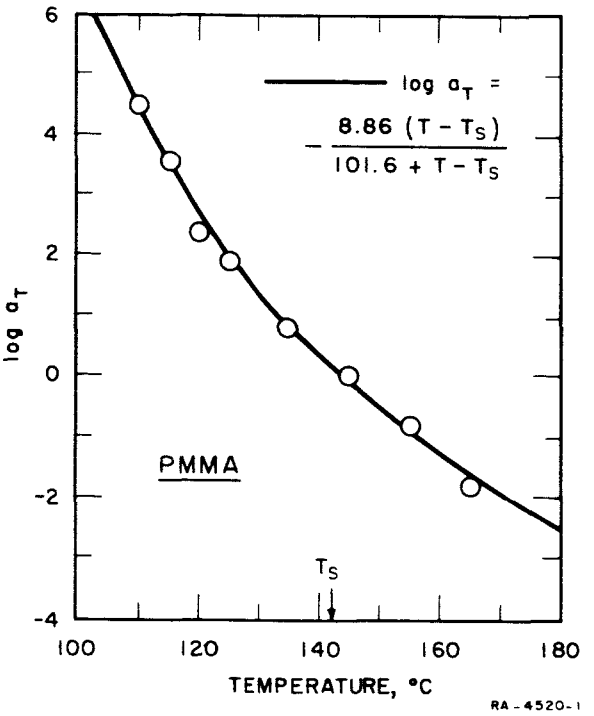

FIG. 13 TEMPERATURE DEPENDENCE OF LOG a_T FOR UNCROSSLINKED PMMA

T_s may be determined from empirically obtained a_T values using Eq. (11), as indicated in Fig. 13. The value of T_s obtained in this way (143°C) is reasonable, although somewhat lower than other values reported for PMMA in the literature.[5]

Shift factors calculated from Eq. (11) with T_s = 143°C were used in preparing plots of log $\sigma T_s/T$ vs. log t/a_T for a number of extension ratios. Several of these plots are shown in Fig. 14 where A is an arbitrary additive constant used to separate the curves for convenience in presentation. It can be seen that the time-temperature superposition is quite good, although some scatter exists in the low temperature data; the 120°C data are somewhat below those at other temperatures. Figure 13 shows that a_T at 120°C also lies below the WLF curve. This suggests that the actual test temperature was slightly higher than 120°C. These 120°C data were therefore disregarded in drawing full curves (Fig. 14) which best represent the data.

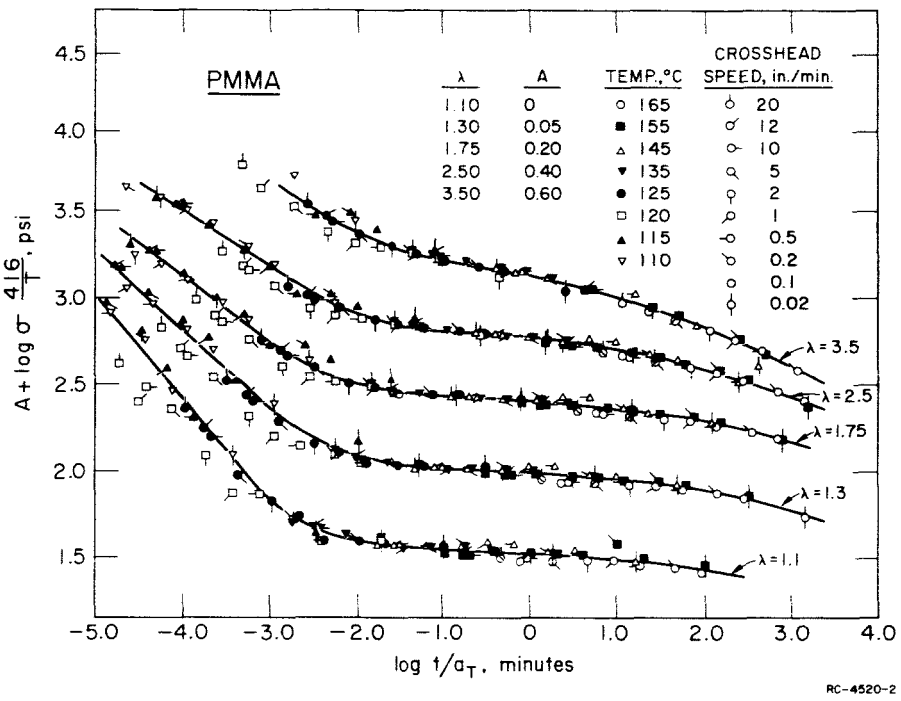

FIG. 14 VARIATION OF (Reduced) STRESS WITH REDUCED TIME AT DIFFERENT STRAIN VALUES FOR UNCROSSLINKED PMMA. Temperature shift factors determined from curve in Fig. 13; $a_T = 1.0$ at 143°C

When curves like those in Fig. 14 are parallel, then the viscoelastic data must conform to Eq. (9). To test the applicability of Eq. (9), isochronal values (values at a constant time) of $\sigma T_s/T$ were read from curves like those in Fig. 14 and are shown in Fig. 15 on plots of log $\lambda\sigma T_s/T$ vs. log $(\lambda-1)$, where $\lambda\sigma$ is the true stress (i.e., stress based on the cross-sectional area of a deformed specimen). An arbitrary additive constant A is again used to separate the curves.

Because the lines in Fig. 15 have a unit slope and are linear up to about 100% extension for $0.001 < t/a_T < 100$ minutes, it follows that under these conditions $g(\lambda)$ from Eq. (9) equals λ. At reduced times less than 0.001 minute, deviations from linearity occur at extensions less than 100%. Because these short times correspond to temperatures relatively near T_g, the result is not surprising and is undoubtedly caused by relaxation modes within individual network chains becoming effective, thus changing the inherent stress-strain response and increasing the modulus.

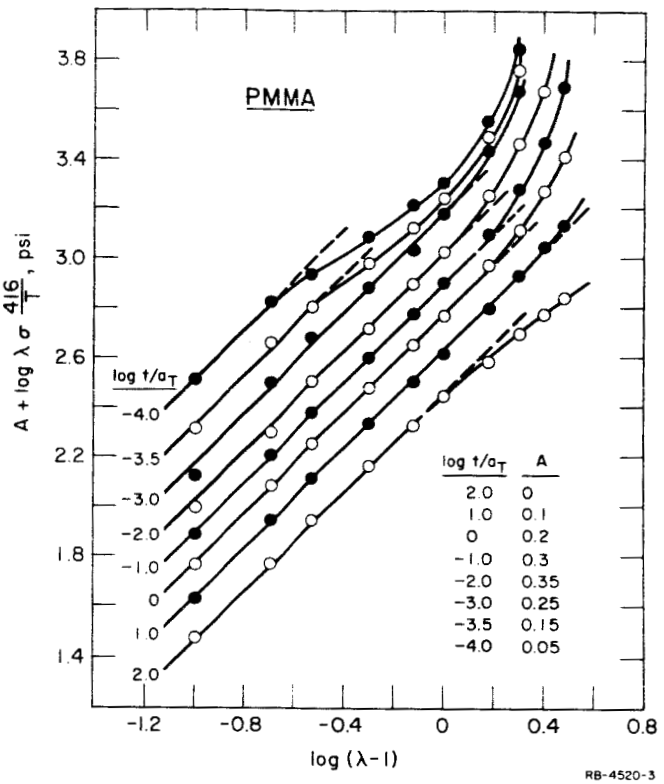

FIG. 15 ISOCHRONAL VALUES OF TRUE STRESS AS A FUNCTION OF STRAIN FOR UNCROSSLINKED PMMA

Since $g(\lambda) = \lambda$ for $\lambda < 2$ at the reduced times at which the curves in Fig. 14 have an extended flat portion, the modulus $F(t)$ can be evaluated directly using Eq. (9). The 10-minute value at 143°C is about 330 psi (2.3×10^7 dynes/cm^2). This modulus characterizes the network formed by the physical entanglement of the chains in the uncrosslinked PMMA.

Figure 16 shows the failure envelope obtained by plotting log $\lambda_b \sigma_b 416/T$ against log $(\lambda_b - 1)$. In those instances that the stress-time curves from Instron tests showed yield values (found at lower temperatures and higher crosshead speeds) or contained an indication of viscous flow during the test (found at higher temperatures and lower crosshead speeds), the break data are eliminated from the plot. However, these data are plotted in Fig. 17.

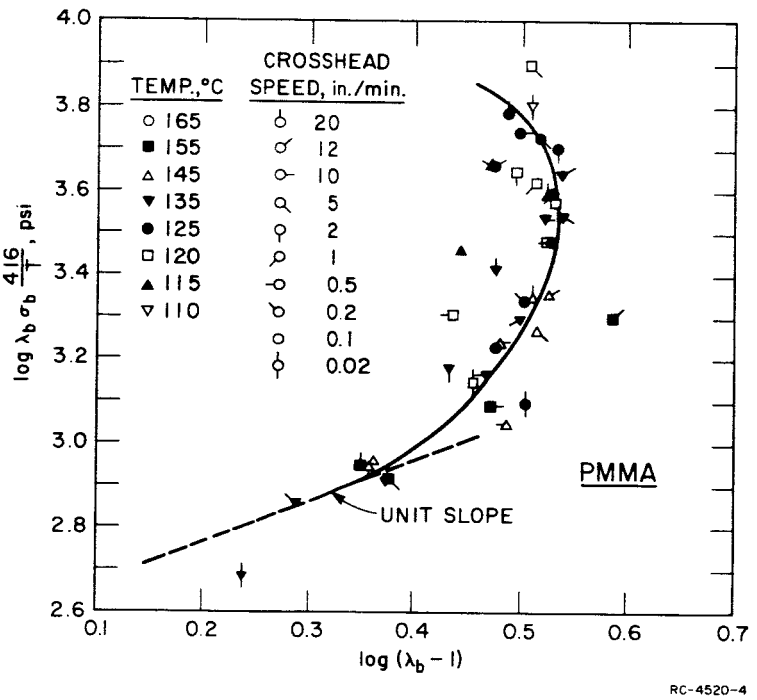

FIG. 16 FAILURE ENVELOPE FOR UNCROSSLINKED PMMA

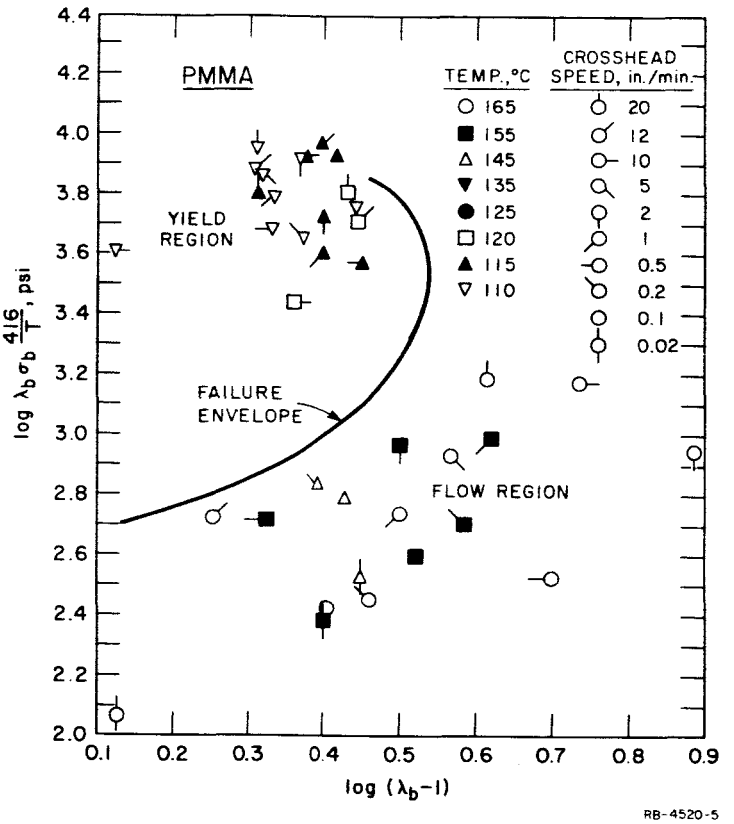

FIG. 17 YIELD AND FLOW BEHAVIOR OUTSIDE OF FAILURE ENVELOPE FOR UNCROSSLINKED PMMA. Failure envelope from Fig. 16

Failure envelopes are usually obtained only on crosslinked polymers. Figure 16 shows that data on an uncrosslinked polymer also yield a failure envelope, although a smaller segment of the envelope is defined because of the flow and yield phenomena. For crosslinked polymers, the lower branch of the failure envelope normally approaches asymptotically the equilibrium stress-strain curve and conforms to the equation: $\log \lambda_b\sigma_b = \log E_e + \log (\lambda_b - 1)$. Uncrosslinked polymers do not have an equilibrium modulus, but if the entanglement coupling density is high, this gives a pseudo-equilibrium modulus, indicated by a relatively flat portion in the modulus vs. time curve. It is interesting to note that the modulus obtained from the unit slope region of the envelope (even though it is not well defined because of the occurrence of flow) is

347 psi, in agreement with the modulus derived from the flat portion of the curves in Fig. 14.

B. Special Samples of Crosslinked PMMA (Ames)

These samples, crosslinked with 0.3 and 0.8% EDMA were tested at various extension rates and temperatures. Figure 18 shows a_T values obtained by superposing plots of log $\sigma 273/T$ vs. log t from data at the different temperatures and at several constant values of λ. For both samples, it appears that T_s = 426°K (153°C), a value somewhat above that (T_s = 416°K) found for the uncrosslinked PMMA sample (see Fig. 13). This behavior is qualitatively in agreement with the findings of Fox and Loshaek[20] concerning the dependence of T_g ($T_s \cong T_g + 50$) on crosslink density.

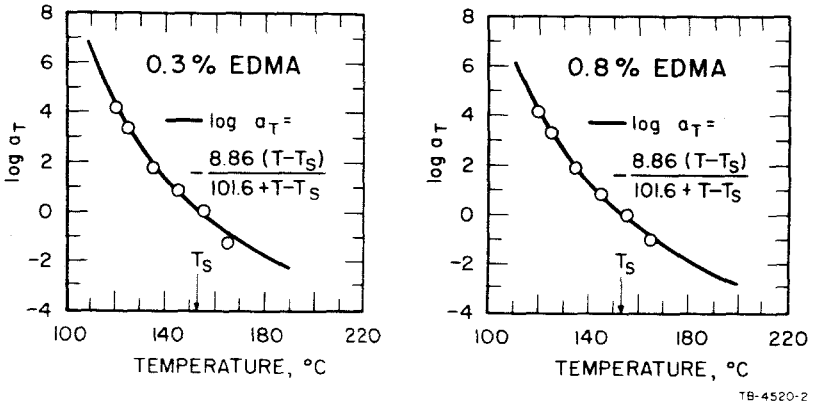

FIG. 18 TEMPERATURE DEPENDENCE OF LOG a_T OBTAINED FOR CROSSLINKED PMMA SAMPLES (AMES) BY SUPERPOSING STRESS-STRAIN DATA

Equation (11) with T_s = 426°K was used to calculate the shift factors employed to construct the master stress-time curves shown in Fig. 19, in which log $\sigma T_s/T$ is plotted against log t/a_T for λ = 1.1, 1.3, 1.75, 2.5, and 3.5. Curves were also prepared for λ = 1.2, 1.5, 2.0, and 3.0, but these are omitted for simplicity. No curves for either sample show a clearly developed flat portion corresponding to the equilibrium modulus. Although this behavior may partially result from chemical relaxation, it more likely results from the slippage of entangled chains or other

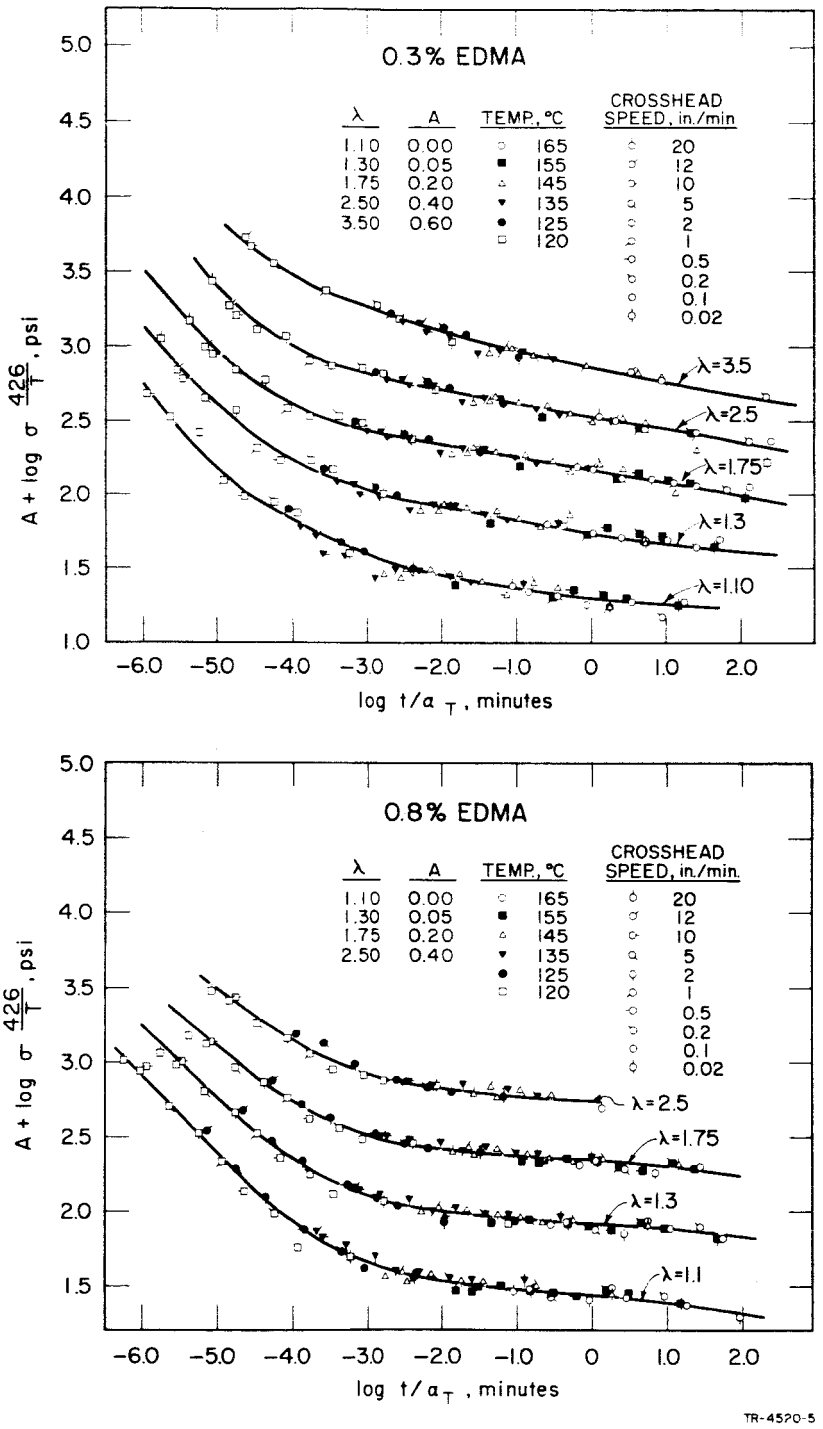

FIG. 19 VARIATION OF (Reduced) STRESS WITH TIME AT DIFFERENT STRAIN VALUES FOR TWO CROSSLINKED PMMA SAMPLES (Ames). Temperature shift factors from curves in Fig. 18

cooperative process which involves clusters of network chains. This long term relaxation phenomenon is also shown by creep data[17] and by the dynamic (complex) shear compliance[16] on various types of vulcanizates. A striking example is provided by stress-strain data on a series of Viton A-HV[3,4] and other[18] vulcanizates crosslinked by different amounts. Bueche[17] has considered the phenomenon in terms of a slow rearrangement of network junction points; the extent and time-scale of the process increase with an increase in the fraction of dangling (inactive) chains. The slippage of entanglement crosslinks has been considered by Kraus and Moczygemba[15] and also by Ferry[16] and his associates.

Isochronal stress-strain data obtained from Fig. 19 are shown in Fig. 20; the data are similar to those for the uncrosslinked PMMA (Fig. 15). From the straight lines of unit slope in Fig. 20, it is found that the 10-minute moduli at 153°C for the samples containing 0.3% and 0.8% EDMA are, respectively, 195 and 288 psi. The 10-minute modulus for the uncrosslinked PMMA (Section IV-A) at 143°C is about 330 psi, a value greater than for the crosslinked polymers. Although the moduli values given here are

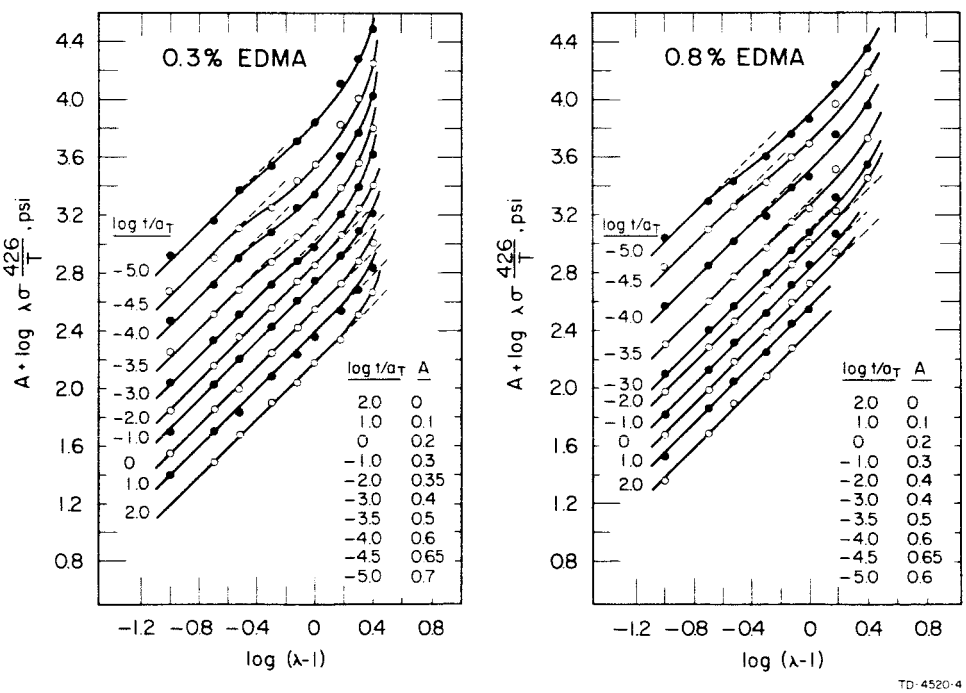

FIG. 20 ISOCHRONAL VALUES OF TRUE STRESS AS A FUNCTION OF STRAIN FOR TWO CROSSLINKED PMMA SAMPLES (Ames)

obtained at different temperatures, the comparison is a reasonably valid one since each modulus was derived from data in the plateau region. Data from Fig. 19 were also used to prepare the plots of log $\sigma(1)/F(1)$ *vs.* log λ shown in Fig. 21. [$\sigma(1)$ and $F(1)$ are the stress and modulus at 1-minute at the temperatures indicated by the legend on Fig. 21.] The solid curve is that given by the strain function, $(\lambda-\lambda^{-2})/3 \equiv \Gamma(\lambda)$, from the statistical theory of rubberlike elasticity.

Ultimate property data from the tests (including those at 110 and 115°C) are assembled in Fig. 22. The lower (high temperature) portions of the failure envelopes are drawn as straight lines with unit slope from which the moduli were estimated to be 174 and 288 psi, in reasonable agreement with 10-minute modulus values of 195 and 287 psi obtained from the data in Fig. 20.

Values of ν_e, estimated by three methods, are given in Table V. (The uncrosslinked sample is that discussed in Section IV-A.) For the

Table V

ESTIMATED VALUES OF ν_e FOR PMMA SAMPLES (AMES)

Amount of Crosslinker g/100 g monomer	Modulus,* psi	$\nu_e \times 10^4$, moles/ml		
		Method A	Method B	Method C
0.3	195	0.359	1.23	0.84
0.8	288	0.953	1.87	1.97
0	330	--	(2.14)	--

Method A: Calculated from amount of crosslinker, as indicated by Eq. (2).

Method B: From $\nu_e=E_e/3RT$

Method C: From swollen stress-strain data obtained at the Ames Research Center

*For the two crosslinked polymers, the moduli are 10-minute values at 153°C; for the uncrosslinked polymer, the modulus is the 10-minute value at 143°C.

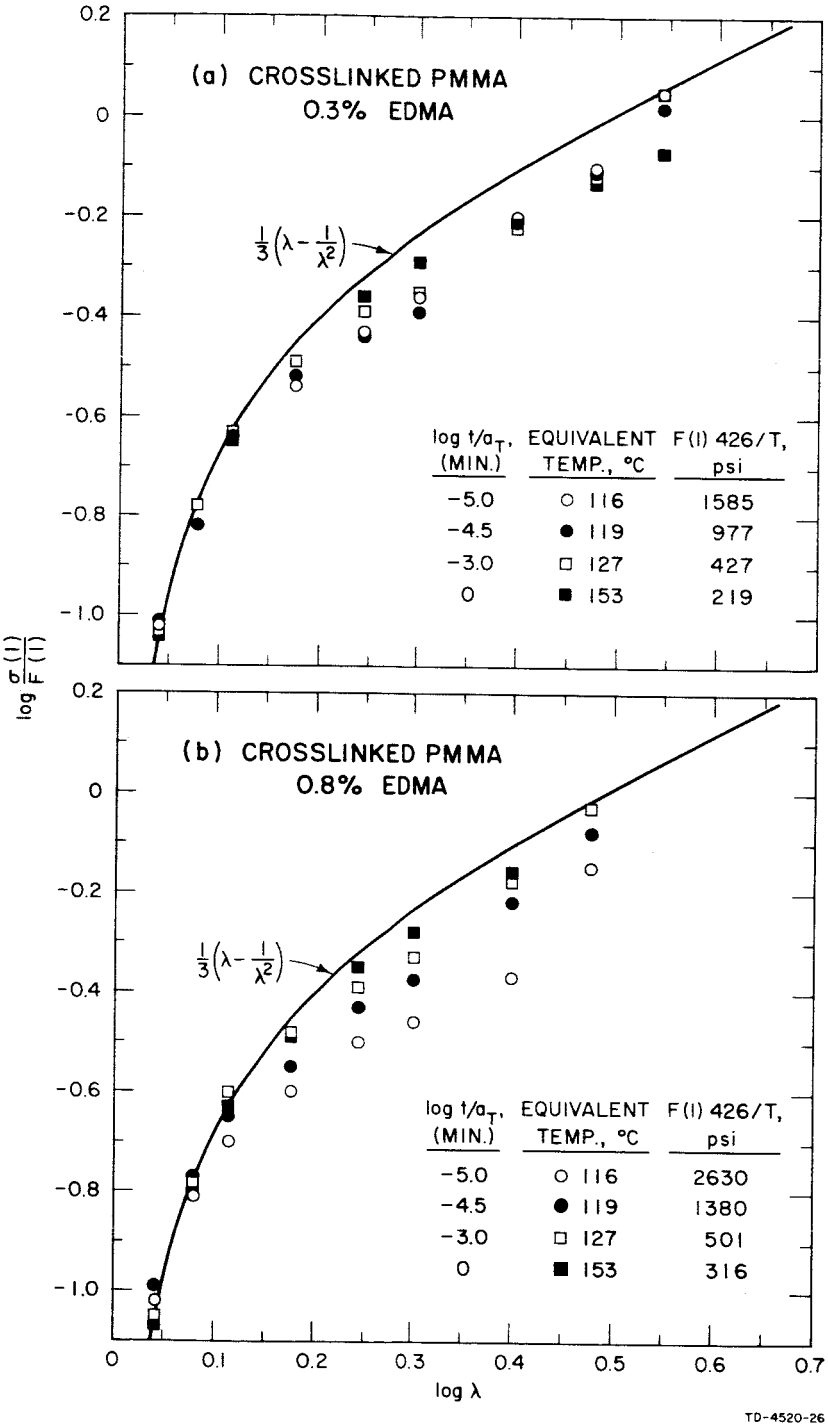

FIG. 21 PLOTS OF LOG $\sigma(1)/F(1)$ vs. LOG λ FOR PMMA POLYMERS (Ames) CROSSLINKED WITH 0.3% AND 0.8% EDMA

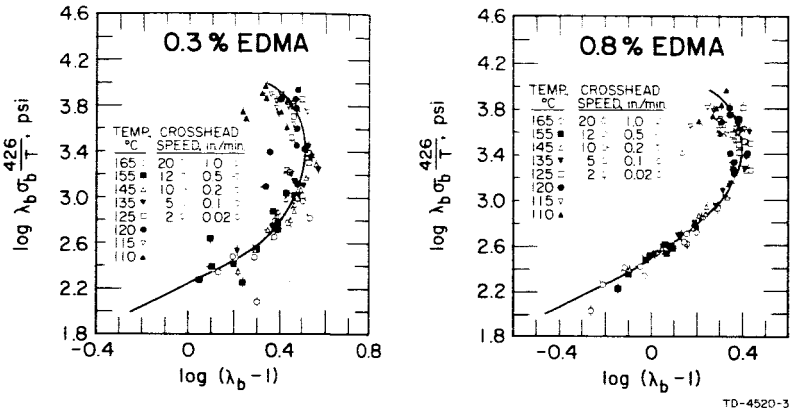

FIG. 22 FAILURE ENVELOPE FOR TWO CROSSLINKED PMMA SAMPLES (Ames)

highest crosslinked sample, Methods B and C give values which are in good agreement. The higher value obtained by Method B for the less densely crosslinked sample is probably caused by the fact that an equilibrium modulus was not obtained from the stress-strain data on dry specimens whereas the data on swollen specimens are probably equilibrium ones. In light of the modulus and swelling data for the Polycast PMMA polymers (see Section II), it is somewhat surprising that the modulus of the lightly crosslinked polymer is only 195 psi. It is possible that impurities terminated growing chains during the polymerization and thus prevented the formation of a highly effective entanglement network.

C. Crosslinked PMMA Samples (Polycast Corp.)

Crosslinked polymers, as well as the uncrosslinked material Lot 1, were tested at various temperatures and extension rates. The derived isochronal data were used to obtain the 1-minute modulus F(1) at each temperature from plots of $\lambda\sigma$ vs. λ-1, as illustrated by Fig. 23. From F(1) and values of the stress at 1-minute, $\sigma(1)$, plots were made of

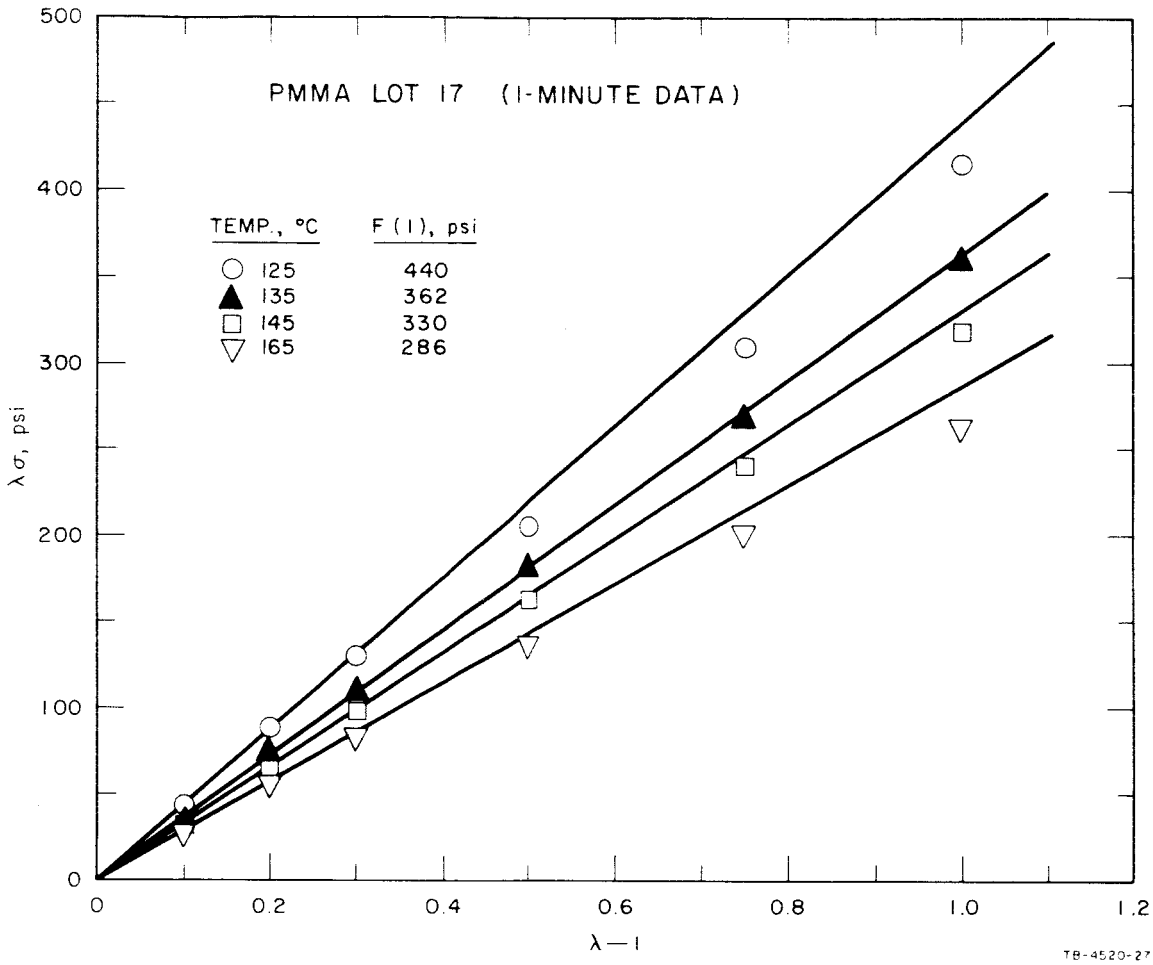

FIG. 23 EXAMPLE OF PLOTS USED TO OBTAIN THE 1-MINUTE CONSTANT-STRAIN-RATE MODULUS FOR THE CROSSLINKED PMMA POLYMERS (Polycast)

log $\sigma(1)/F(1)$ vs. log λ, as illustrated by Figs. 24 and 25. Because the highly crosslinked samples, Lots 4 and 12, broke at quite low extensions, the stress-strain data are not highly precise and were only partially analyzed.

Typical failure envelopes are shown in Fig. 26, and failure envelopes for all of the crosslinked samples are shown, without points, in Fig. 27.

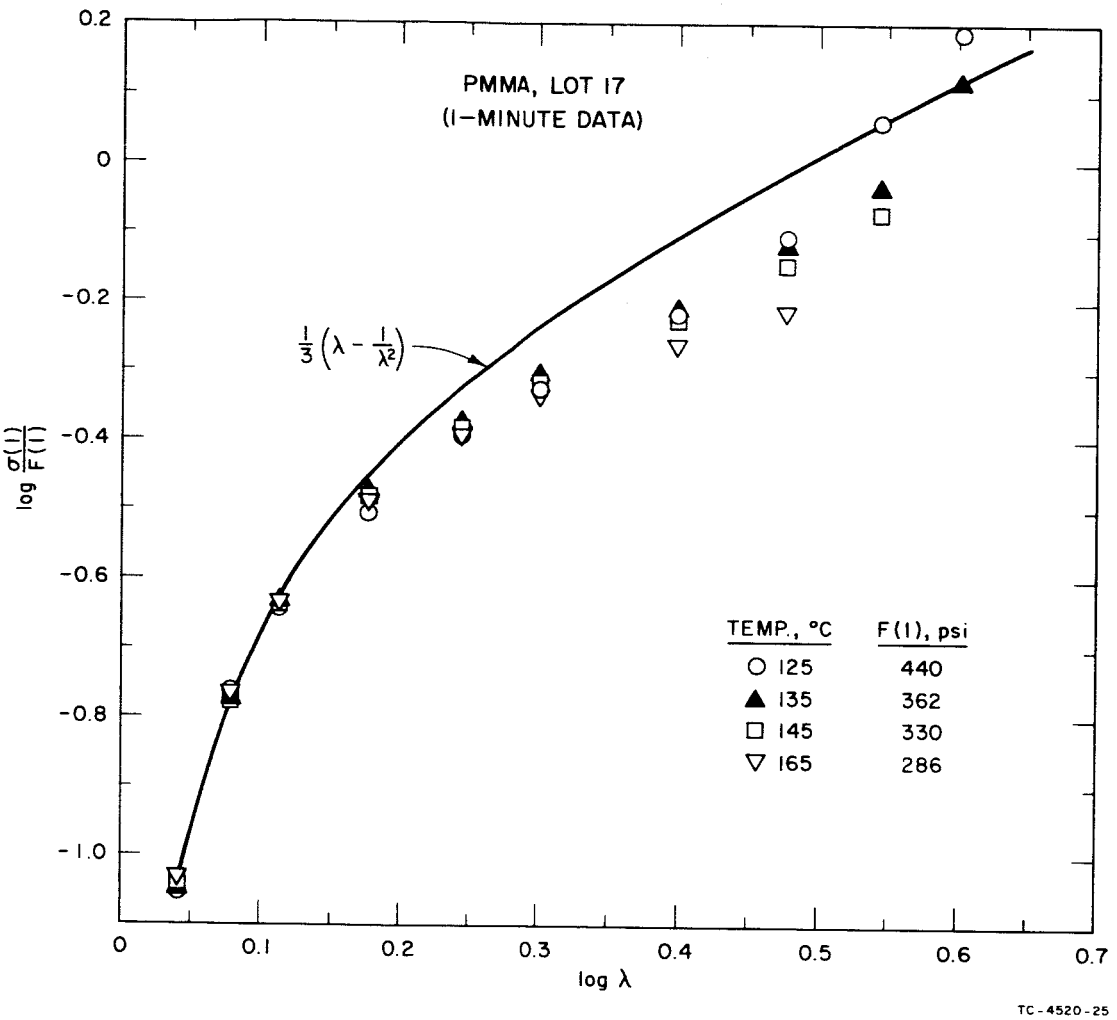

FIG. 24 PLOTS OF LOG $\sigma(1)/F(1)$ vs. LOG λ FOR CROSSLINKED PMMA, LOT 17, AT 125, 135, 145, AND 165°C

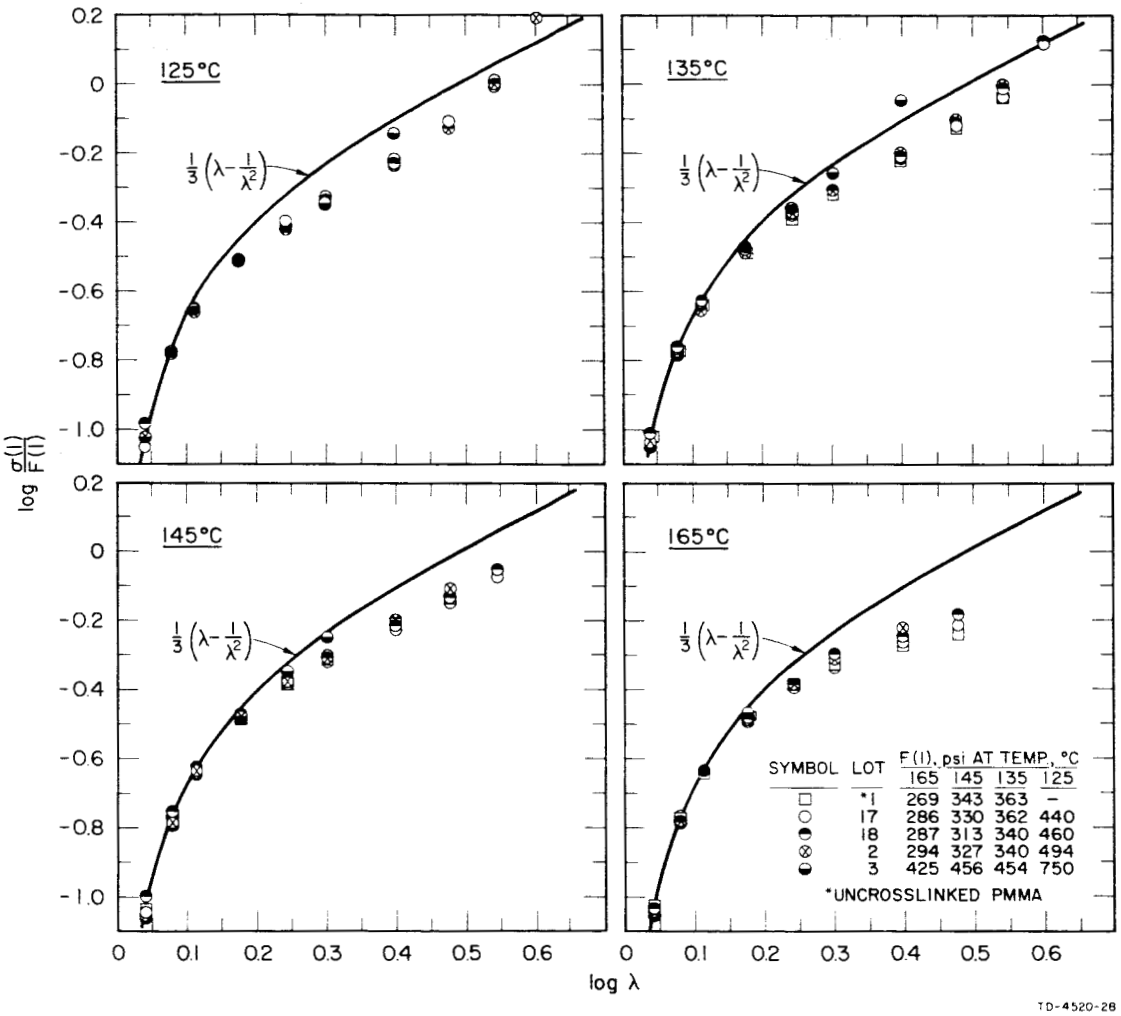

FIG. 25 PLOTS OF LOG $\sigma(1)/F(1)$ vs. LOG λ OF PMMA POLYMERS OF DIFFERENT CROSSLINK DENSITIES AT TEMPERATURES BETWEEN 125 AND 165°C

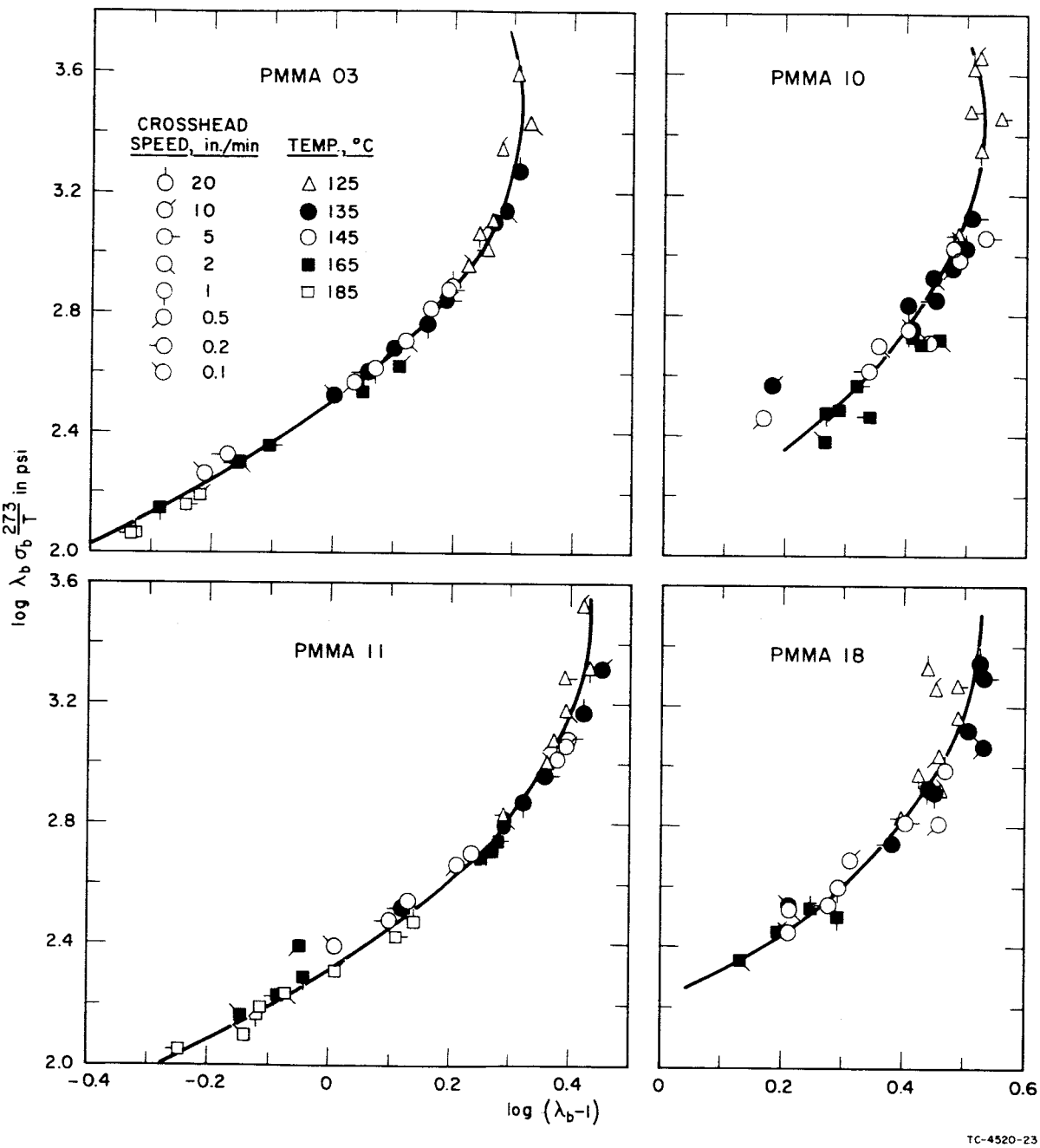

FIG. 26 FAILURE ENVELOPES FOR CROSSLINKED PMMA POLYMERS. (Lots 3 and 18, EDMA-crosslinked; Lots 10 and 11, HDMA-crosslinked)

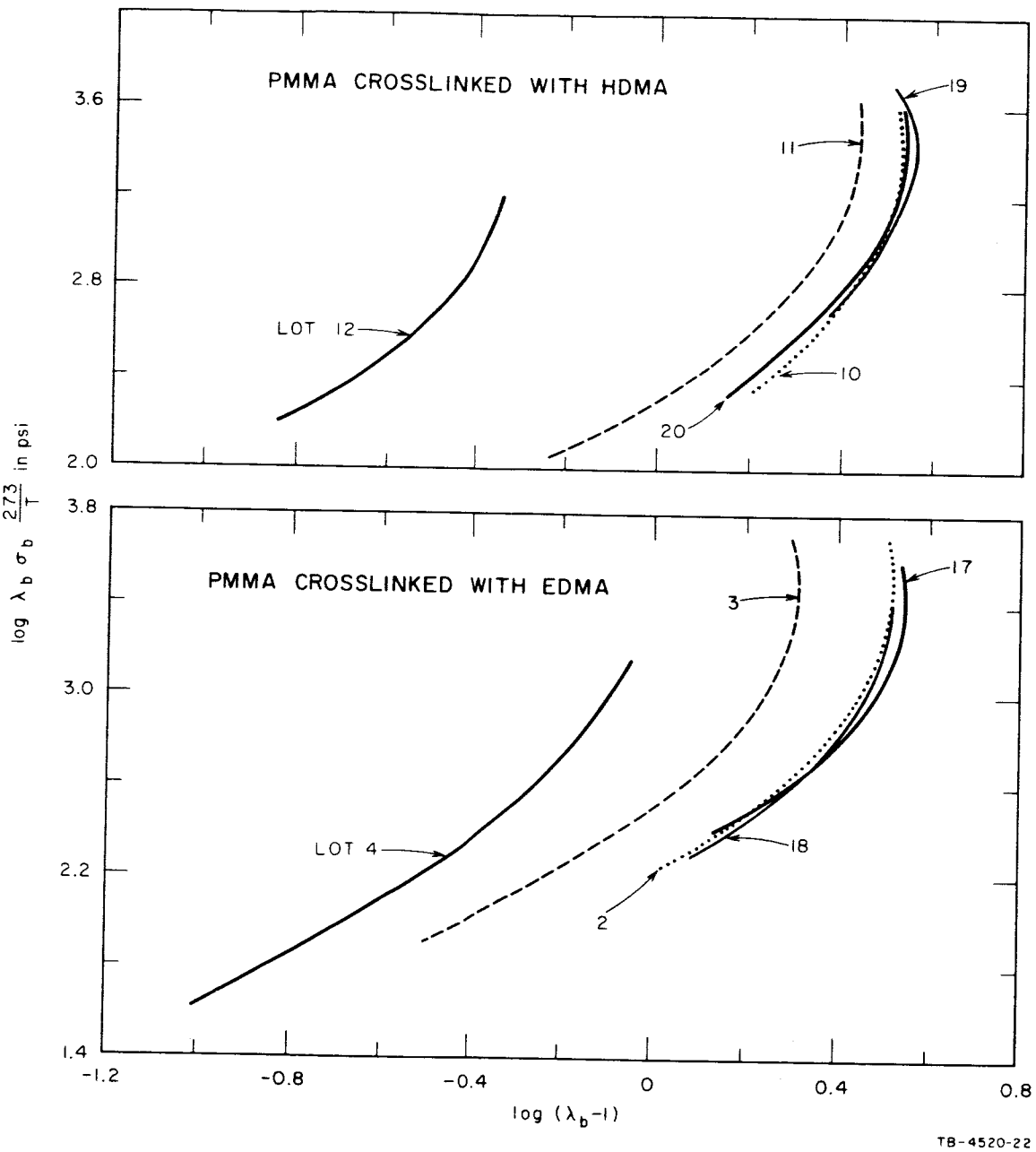

FIG. 27 FAILURE ENVELOPES FOR ALL CROSSLINKED PMMA POLYMERS (Polycast)

D. Discussion of Results

1. Ultimate Tensile Properties

The failure data in Figs. 16, 22, and 26 show that each PMMA exhibits its maximum extensibility, $(\lambda_b)_{max}$, at about 125°C at the extension rates used. According to current viewpoints,[14,11] the values of λ_b are smaller at temperatures below 125°C because the network chains do not respond as a single unit. Instead, sub-molecules of the chain respond, thus causing the extensibility to be reduced and the tensile strength, σ_b, to be increased. As discussed by Halpin,[14] the effective length of the chain is reduced as the glass temperature is approached.

The failure envelopes in Fig. 27, except that for Lot 4, have nearly the same shapes, and the true stress, $\lambda_b\sigma_b 273/T$, at $(\lambda_b)_{max}$ is the same for all samples within the experimental uncertainty. Thus, the envelopes can be superposed reasonably well by shifting them along the abscissa. Similar behavior has been found[11,19c] for a series of Viton A-HV (hydrofluorocarbon) gum vulcanizates. One difference is the magnitude of $(\lambda_b\sigma_b)_{max}$, the non-temperature-reduced true stress at $(\lambda_b)_{max}$: for the Viton A-HV vulcanizates, this value is about 2.5-fold greater than that for the PMMA elastomers. (Although this relative value for $(\lambda_b\sigma_b)_{max}$ is only semi-quantitative because of the considerable difficulty in obtaining a precise value for the stress at $(\lambda_b)_{max}$, it does appear that $(\lambda_b\sigma_b)_{max}$ for the two types of elastomers differs considerably.)

Plots which show the dependence of $\sigma_b 273/T$ and of λ_b on the reduced time-to-break, t_b/a_T, were prepared from data at temperatures between 125 and 185°C on Lot 11. Values of log a_T obtained from superposing the $\sigma_b 273/T$ and the λ_b data are shown in Fig. 28 plotted against 1/T; they yield a rather good straight line on the Arrhenius-type plot whose slope corresponds to an activation energy of 46 Kcal. The a_T values definitely do not conform to the WLF equation. Values of a_T for superposing ultimate property data for vulcanizates of SBR[21] (styrene-butadiene), Viton B,[22,7] butyl[7] (sulfur-cured) vulcanizates and for rubbery epoxy resins[23] and solid propellants[24] have been found to agree rather well with the WLF equation.

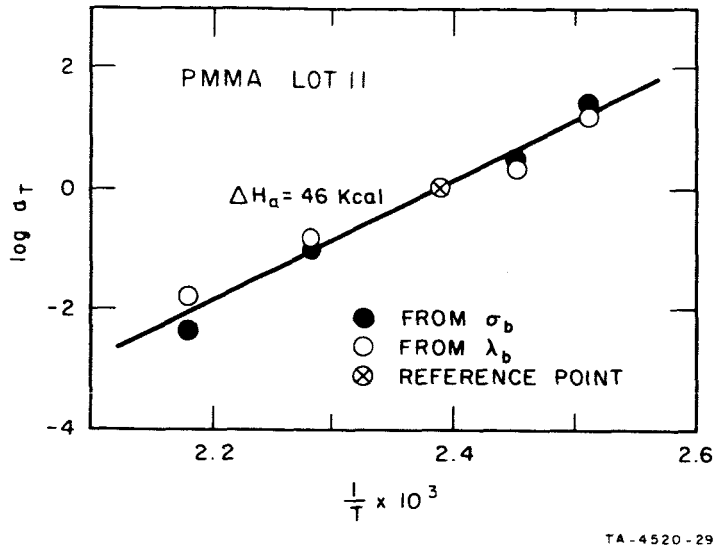

FIG. 28 TEMPERATURE DEPENDENCE OF LOG a_T OBTAINED BY SUPERPOSING ULTIMATE PROPERTY DATA ON CROSSLINKED PMMA, LOT 11

However, for a silicone vulcanizate[7] (T_g = -125°C) and a Viton A-HV (A-6) vulcanizate,[25] a_T conforms to an Arrhenius type equation. This behavior is perhaps not unexpected since the test temperatures extended up to $T-T_g$ = 225°C for the silicone vulcanizate and to $T-T_g$ = 256°C for the Viton vulcanizate. Normally, the WLF equation is applicable at temperatures for which $T-T_g$ is less than 100° or possibly 150°C. However, for styrene-butadiene and ethylene-propylene vulcanizates containing different amounts of carbon black, it has been found[26] that a_T values from superposing ultimate property data obey the Arrhenius equation. Thus, until the controlling step in rupture is better understood in terms of viscoelastic processes, some caution is warranted in superposing ultimate property data by using a_T values based on the WLF equation, unless the data clearly indicate that this equation is applicable.

Values of a_T from the line in Fig. 28 were used in preparing the reduced plots in Fig. 29. Although the points scatter somewhat, the scatter is not much worse than commonly found upon superposing ultimate property data.

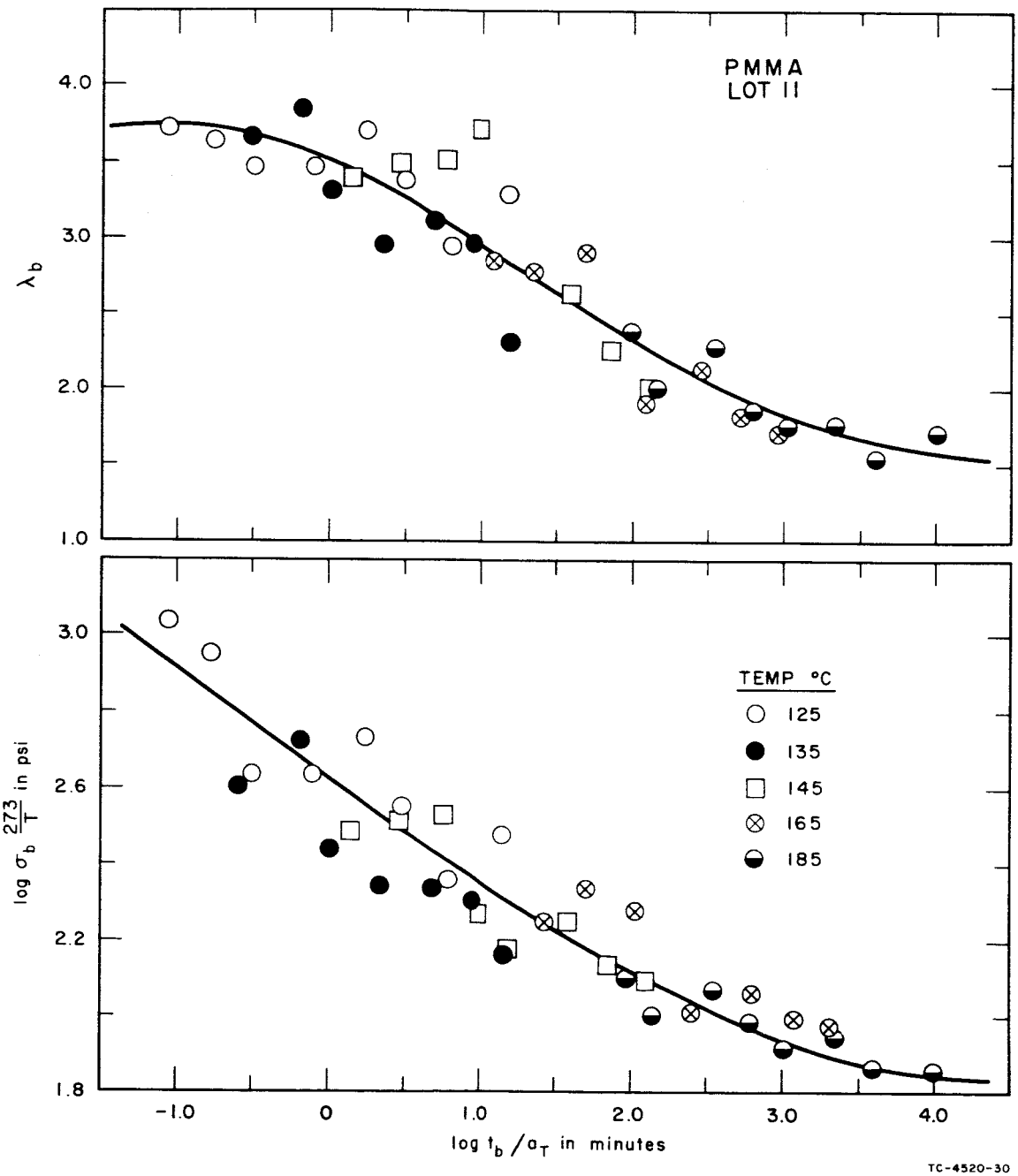

FIG. 29 PLOTS OF LOG $\sigma_b 273/T$ AND OF λ_b AGAINST LOG t_b/a_T FOR CROSSLINKED PMMA, LOT 11. $a_T = 1$ at 145°C

A comparison was made of plots of log $\sigma_b 273/T$ vs. log t_b/a_T for a number of elastomers; curves for different vulcanizates were shifted along the abscissa so that each vulcanizate was in a corresponding state. (This was done by adjusting t_b/a_T so that $(\lambda_b)_{max}$ for each vulcanizate occurred at the same value of t_b/a_T.) The comparison showed quite clearly that σ_b for the PMMA sample was significantly less at all values of t_b/a_T than for the other vulcanizates. Although the reason for this behavior is not known, it may be related in some manner to the characteristic features of PMMA chains which causes the chains to form a considerably more tightly crosslinked entanglement network than do chains of other polymers (see Table 13-II in Ref. 5).

A discussion has been given,[11] which includes considerations of previous work, of the dependence of $(\lambda_b)_{max}$ on the length (molecular weight) of network chains. If a network deforms affinely at all deformations up to rupture, then theoretical considerations show that $(\lambda_b)_{max} \propto M_c^{\frac{1}{2}}$, provided $(\lambda_b)_{max} \propto (\lambda_\infty)_{max}$. Because of inherent difficulties in obtaining reliable values for M_c, a satisfactory evaluation has not been made of the dependence of $(\lambda_b)_{max}$ on $M_c^{\frac{1}{2}}$ for any vulcanizates. Data on a series of Viton A-HV vulcanizates suggest[11] that $(\lambda_b)_{max} \propto M_c^{0.7}$ for these vulcanizates.

Figure 30 shows a plot of log $(\lambda_b)_{max}$ vs. log F(1) for the PMMA polymers, where F(1) is the modulus at 165°C; for the "Ames" polymers, 10-minute modulus values at 153°C are used (see Table V). If the modulus is proportional to ν_e, then Fig. 30 indicates that $(\lambda_b)_{max} \propto \nu_e^{-0.9}$, at least for the more highly crosslinked polymers. Figure 31 shows a plot of log $(\lambda_b)_{max}$ vs. log $(\nu_e)_{sw}$, where $(\nu_e)_{sw}$ was obtained from equilibrium swelling data.

2. Stress-Strain Characteristics

An examination of plots of log σ vs. log t indicated that the curves at different temperatures could be superposed to give master plots like those shown for the uncrosslinked PMMA and the crosslinked PMMA polymers in Figs. 14 and 19. However, instead of considering the time dependence directly, attention was given to the stress-strain characteristics as

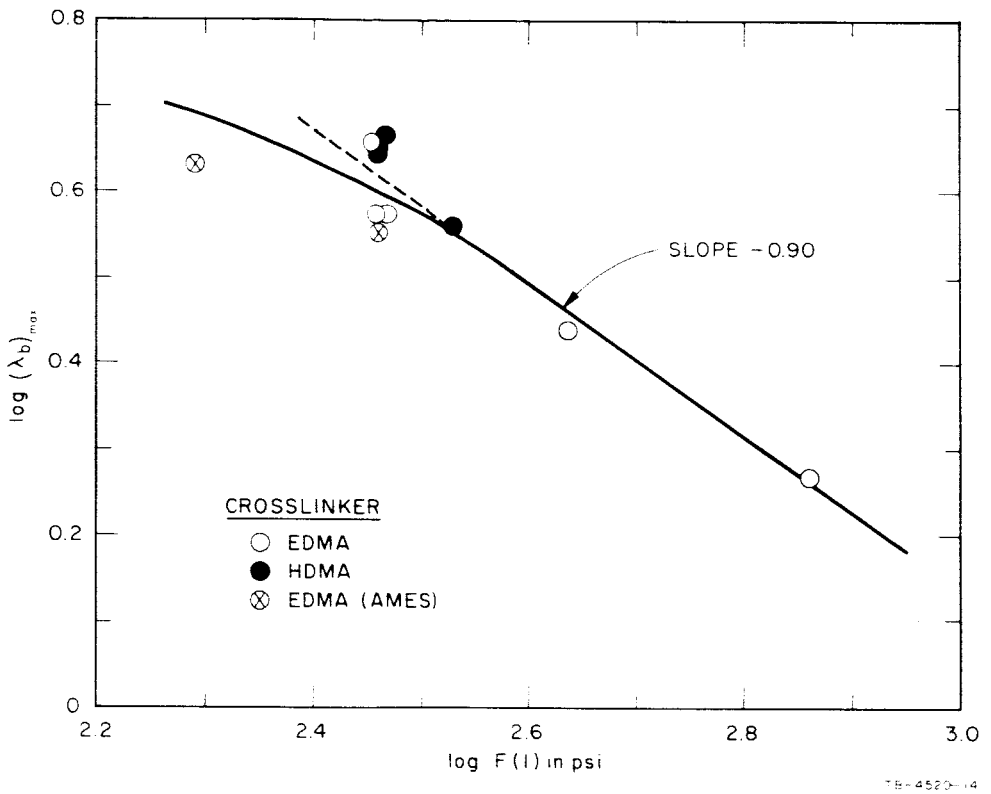

FIG. 30 PLOT OF LOG $(\lambda_b)_{max}$ vs. LOG F(1) FOR CROSSLINKED PMMA POLYMERS (Polycast). F(1) is the 1-minute modulus at 165°C

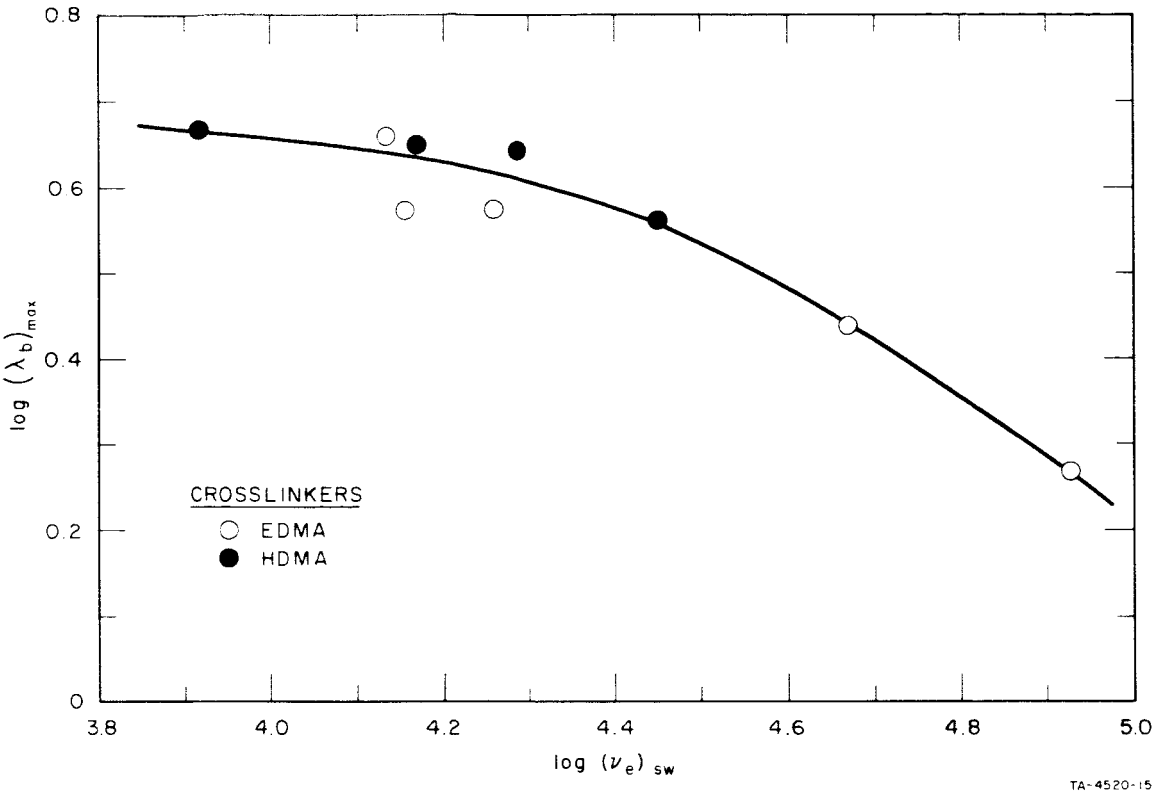

FIG. 31 PLOT OF LOG $(\lambda_b)_{max}$ vs. LOG $(\nu_e)_{sw}$ FOR CROSSLINKED PMMA POLYMERS (Polycast). $(\nu_e)_{sw}$ is the moles of effective network chains per unit volume derived from equilibrium swelling data

shown by plots of $\Gamma(\lambda) \equiv \sigma(\lambda,t)/F(t)$ vs. λ. Because polymeric materials show linear viscoelastic behavior at small deformations, $\Gamma(\lambda)$ will approach the strain $(\lambda-1)$ in the limit of zero strain, regardless of test conditions and polymer characteristics. At large deformations, $\Gamma(\lambda)$ shows the network response characteristic at a constant value of time. The response characteristic can be compared, for example, with that predicted by the statistical theory of equilibrium elasticity. The response (or strain) function from this theory is $\Gamma(\lambda) \equiv \sigma/E_e = (\lambda-\lambda^{-2})/3$, where E_e is the equilibrium tensile modulus given by $E_e = 3G = \nu RT$.

Although for many rubber vulcanizates $\Gamma(\lambda)$ is time- and temperature-independent over rather extended ranges of these variables, it is dependent on test conditions for certain vulcanizates. To illustrate the temperature dependence of $\Gamma(\lambda) \equiv \sigma(\lambda,t)/F(t)$, 1-minute data for a Viton A-HV vulcanizate

are shown in Fig. 32. For this rubber vulcanizate, the modulus $F(1)273/T$ increases from 58 to 442 psi as the temperature is reduced from 230 to -5°C; yet, the ratio $\sigma(1)/F(1)$ is sensibly temperature independent for extensions up to about 60%. However, as the extension increases, the values become somewhat less than those given by the statistical theory expression, $(\lambda-\lambda^{-2})/3$. At intermediate extensions, the deviation from $(\lambda-\lambda^{-2})/3$ at a prescribed λ increases as the temperature is decreased from 230 to 25°C.

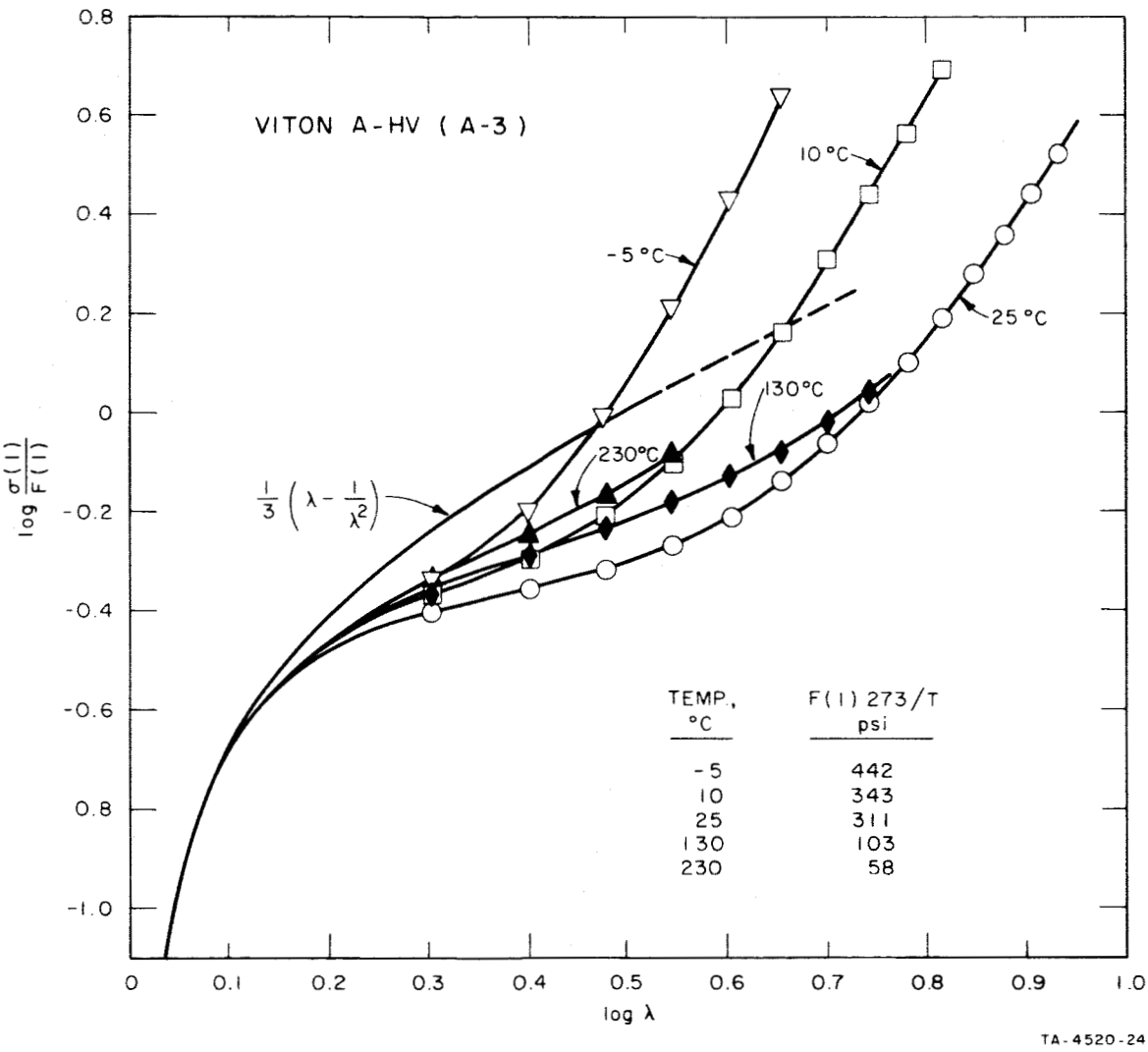

FIG. 32 PLOT OF LOG $\sigma(1)/F(1)$ vs. LOG λ FOR VITON A-HV (A-3) VULCANIZATE SHOWING DATA AT SELECTED TEMPERATURES BETWEEN -5 AND 230°C

At temperatures below 25°C, the maximum extensibility $(\lambda_\infty)_{max}$ decreases with a temperature decrease (discussed in Section IV-D-1). At temperatures above 25°C, $(\lambda_\infty)_{max}$ may be somewhat temperature-dependent. Data on Viton A-HV vulcanizates crosslinked by different amounts show[3,4] that the deviation of $\sigma(1)/F(1)$ from $(\lambda-\lambda^{-2})/3$ becomes less with an increase in crosslink density. This behavior is in agreement with that shown by other vulcanizates and discussed by Halpin.[18]

Values of $\sigma(1)/F(1)$ for the PMMA sample, Lot 17 (Fig. 24) are nearly temperature-independent between 125 and 165°C; however, the deviation from $(\lambda-\lambda^{-2})/3$ does become slightly less as the temperature is decreased. The dependence of $\sigma(1)/F(1)$ on crosslink density and temperature is shown by the data in Fig. 25. Generally speaking, an increase in crosslink density leads to a reduction in the deviation of $\sigma(1)/F(1)$ from $(\lambda-\lambda^{-2})/3$; likewise, the deviation decreases as the temperature is reduced from 165 to 135°C. In these plots, certain points for the more highly crosslinked samples at large extensions lie close to and above the theoretical curve because of finite extensibility effects.

In contrast to the Viton A-HV vulcanizates, $\sigma(1)/F(1)$ for the PMMA polymers (Polycast) is relatively independent of temperature and crosslink density. On the other hand, owing to the entanglement network in the PMMA polymers, the effective crosslink densities (as given by $F(1)$ at 165°C) of all polymers whose properties are shown in Fig. 25 differ by less than a factor of two. However, the slight dependence of $\sigma(1)/F(1)$ on temperature and crosslink density is opposite to that shown by the Viton A-HV vulcanizates above 25°C. (A consideration of the temperatures at which the PMMA and Viton A-HV polymers show their maximum extensibility suggests that it is valid to compare data on the PMMA polymer at temperatures above about 125°C with those on the Viton A-HV polymers above 25°C.)

Figure 21 shows that the Ames PMMA polymers behave differently than the ones from Polycast (Figs. 24 and 25). For the Ames polymers, the deviation of $\sigma(1)/F(1)$ from $(\lambda-\lambda^{-2})/3$ increases as the temperature is reduced. However, the deviation is less for the sample containing 0.3% EDMA than for the one containing 0.8% EDMA.

From the results shown, new conclusions have not yet been drawn about relations between structural factors and the inherent shape of the stress-strain curve. The material presented was based on a first-approximation type of analysis. A refined analysis would require an estimate to be made of the maximum extensibility (the hypothetical value in the absence of rupture) at each temperature. These values would permit a comparison to be made of the $\Gamma(\lambda)$ data, at all extensions and temperatures, at those values of λ which represent equal fractions of the maximum extensibility.

V SUMMARY

Continuous and intermittent stress-relaxation data were obtained on a number of PMMA polymers crosslinked with ethylene glycol dimethacrylate (EDMA) and with hexamethylene glycol dimethacrylate (HDMA). Data were obtained under vacuum (ca. 1 micron) at temperatures up to about 245°C; tests were also made under atmospheric conditions, primarily at 181°C, and under helium at 222°C. The results show that no chains--or at least relatively few--form during degradation and that the EDMA- and HDMA-crosslinked polymers have stability characteristics which are essentially identical under all test conditions.

Relaxation data under vacuum at 225°C show that effective network chains do not break during periods exceeding 1000 minutes, even though weight losses up to 14% (possibly more) were observed. Results from tests in helium and vacuum environments were sensibly identical and thus the rapid degradation observed under atmospheric conditions at 180-200°C is caused by oxygen.

The stress was observed to decay exponentially with time at 245°C. Such results on four polymers whose crosslinker concentrations differ by six-fold gave a rate constant for chain scission which is sensibly independent of crosslinker concentration. However, weight losses (from initial and final weights of specimens) were found to range up to 63% and to increase with a decrease in crosslinker concentration. Although these findings are consistent with the assumption that chemical junction points in the network effect the termination of a depolymerizing chain, this behavior is unlikely and is at variance with published data. An explanation for the present results is not given. However, a significant fraction of the weight loss during the early stage of decomposition can arise from the decomposition of sol, which unquestionably contains a higher concentration of double bonds than the network.

Tensile stress-strain data were obtained at various constant extension rates on crosslinked and uncrosslinked PMMA polymers at temperatures

between about 125 and 185°C. Derived values of the 1-minute modulus at 165°C, even though they were not equilibrium ones, were considered to be proportional--as a first approximation--to the effective crosslink density. Except for several polymers containing a high concentration of crosslinker, the moduli of the crosslinked and uncrosslinked polymers were almost identical. This behavior shows that the PMMA polymers have a high density of entanglement junction points. Because of this tight entanglement coupling, a chemical crosslinking agent has little effect on the modulus at 165°C unless its concentration is sufficiently great to give chains which have a lower molecular weight than those in the entanglement network. To obtain another measure of crosslink density, equilibrium swelling measurements were made on the crosslinked polymers in two solvents. The results show that some entangled chains are disrupted during swelling, although the final swollen polymers still contain a large fraction of permanently entangled chains.

Time-temperature superposition was applied to data obtained at extensions up to 250% on an uncrosslinked and two crosslinked PMMA polymers. In this way plots were obtained of log $\sigma T_0/T$ vs. log t/a_T; for each curve stress values are at the same extension ratio. Values of the temperature shift factor, a_T, obtained by superposing data, were found to conform to the WLF equation. From the reduced curves, the nonlinear strain function $\Gamma(\lambda)$, which equals the stress divided by the modulus evaluated at zero strain, was obtained as a function of either time or temperature; at large values of λ, the function depends somewhat on the time or temperature.

The strain function $\Gamma(\lambda)$ was also derived from 1-minute stress-strain data for a number of PMMA polymers crosslinked with EDMA and HDMA. The results were compared with the strain function, $(\lambda-\lambda^{-2})/3$, given by the statistical theory of rubberlike elasticity. Except for extensions at which finite extensibility effects become important, the comparison showed that $\Gamma(\lambda)$ is somewhat less than $(\lambda-\lambda^{-2})/3$, and that the stress-strain characteristics are quite similar to those for many conventional rubber vulcanizates. It was found that $\Gamma(\lambda)$ depends to some degree on temperature and crosslinker--especially at large extensions. For the

majority of the polymers studied, $\Gamma(\lambda)$ tends to approach $(\lambda-\lambda^{-2})/3$ as either the temperature is reduced or the crosslinker concentration is increased. The effect of the finite extensibility of chains on $\Gamma(\lambda)$ was not specifically considered. Also, the results did not lead to an explanation for the deviation between $\Gamma(\lambda)$ and $(\lambda-\lambda^{-2})/3$ or for the dependence of the deviation on temperature and crosslinker concentration. However, because of the high concentration of entangled chains, the results might be expected to be insensitive to the crosslinker concentration.

Ultimate property data were used to prepare time- and temperature-independent failure envelopes given by plots of $\log \lambda_b \sigma_b T_o/T$ vs. $\log (\lambda_b-1)$. The shape of the resulting envelopes were found to be sensibly independent of the crosslinker concentration, and thus they can be superposed, within the experimental uncertainty, by shifting them along the abscissa. The maximum extensibility, $(\lambda_b)_{max}$, obtained from each failure envelope, was found to depend on the 1-minute modulus, $F(1)$, at 165°C according to: $(\lambda_b)_{max} \propto [F(1)]^{-0.9}$. This dependence is only an approximate one, and for low values of the modulus, $(\lambda_b)_{max}$ is less dependent on $F(1)$.

Time-temperature reduction was applied to superpose ultimate property data for one crosslinked polymer. The obtained shift factors follow the Arrhenius-type equation and give an activation energy of about 46 Kcal. This behavior, which has also been found for several other elastomers, indicates that a_T values from the WLF equation are not always applicable to superpose ultimate property data.

ACKNOWLEDGMENTS

The authors wish to acknowledge the contributions of P.R. Nelson who constructed the load cells and also assisted in the assembly and operation of the vacuum relaxometer, of C.M. McCullough who contributed to the design of the relaxometer, and of J.A. Rinde who characterized the crosslinked PMMA polymers by equilibrium swelling measurements.

REFERENCES

1. P.J. Flory and J. Rehner, Jr., J. Chem. Phys. 11, 521 (1943); also, P.J. Flory, ibid. 18, 108 (1950).

2. J.C.H. Hwa, J. Polymer Sci. 58, 715 (1962).

3. T.L. Smith, J. Polymer Sci. (submitted).

4. T.L. Smith, Biaxial and Uniaxial Tensile Properties of Elastomers, Technical Report AFML-TR-65-356, October 1965; prepared for the Air Force Materials Laboratory, Wright-Patterson Air Force Base, under Contract No. AF 33(657)-8186.

5. J.D. Ferry, Viscoelastic Properties of Polymers, John Wiley and Sons, Inc., New York, 1961.

6. A.V. Tobolsky, Properties and Structure of Polymers, John Wiley and Sons, Inc., New York, 1960.

7. T.L. Smith, Mechanisms of Reversible and Irreversible Loss of Mechanical Properties of Elastomeric Vulcanizates Which Occur at Elevated Temperatures, Technical Documentary Report No. ASF-TDR-62-572, June 1962. Prepared for the Directorate of Materials and Processes, Wright-Patterson Air Force Base, under Contract No. AF 33(616)-8298.

8. T.L. Smith, Ultimate Tensile Properties of Gum Vulcanizates and Their Temperature Dependence, Technical Documentary Report No. ASD-TDR-63-430, May 1963. Prepared for the Directorate of Materials and Processes, Wright-Patterson Air Force Base, under Contract No. AF 33(657)-8186.

9. S.L. Madorsky, J. Polymer Sci. 11, 491 (1953).

9a. N. Grassie, Chemistry of High Polymer Degradation Processes, Interscience Publishers, Inc., New York, 1956.

9b. J.E. Clark and H.H.G. Jellinek, "Thermal Degradation of Polymethylmethacrylate in a Closed System," in Proceedings of the Battelle Symposium on Thermal Stability of Polymers, Battelle Memorial Institute, Columbus, Ohio, 1963.

9c. N. Grassie and H.W. Melville, Proc. Roy. Soc. A199, 39 (1949).

10. L.R.G. Treloar, The Physics of Rubber Elasticity, 2nd ed., Oxford University Press, London, 1958.

11. T.L. Smith and J.E. Frederick, J. Appl. Phys. 36, 2996 (1965).

12. L. Mullins and A.G. Thomas, "Theory of Rubber-Like Elasticity," Chapt. 7 in The Chemistry and Physics of Rubber-Like Substances, edited by L. Bateman, John Wiley and Sons, Inc., New York, 1963.

13. T.L. Smith, Trans. Soc. Rheology 6, 61 (1962).

14. J.C. Halpin, J. Appl. Phys. 36, 2975 (1965).

15. G. Kraus and G.A. Moczygemba, J. Polymer Sci. A2, 277 (1964).

16. E. Maekawa, R.G. Mancke, and J.D. Ferry, J. Phys. Chem. 69, 2811 (1965); also, previous papers on the same subject co-authored by J.D. Ferry.

17. F. Bueche, J. Appl. Polymer Sci. 1, 240 (1956); also see Chapt. 6 in Physical Properties of Polymers, Interscience, 1962.

18. J.C. Halpin, J. Polymer Sci. (submitted); also review article to be published in Rubber Reviews of Rubber Chem. and Tech.

19. T.L. Smith, (a) J. Polymer Sci. A1, 3597 (1963); (b) J. Appl. Phys. 35, 27 (1964); (c) Proc. of the 4th International Congress on Rheology, edited by E.H. Lee, John Wiley and Sons, Inc., New York, 1965. Part 2, p. 525.

20. T.G. Fox and S. Loshaek, J. Polymer Sci. 15, 371 (1955).

21. T.L. Smith, J. Polymer Sci. 32, 99 (1958).

22. T.L. Smith, J. Appl. Phys. 35, 27 (1964).

23. D.H. Kaelble, J. Appl. Polymer Sci. 9, 1213 (1965).

24. R.F. Landel and T.L. Smith, American Rocket Society Journal 31, 599 (1960).

25. T.L. Smith, Characterization of Ultimate Tensile Properties of Elastomers, Technical Documentary Report No. ML-TDR-64-264, August 1964. Prepared for Air Force Materials Laboratory, Wright-Patterson Air Force Base, under Contract No. AF 33(616)-8298.

26. J.C. Halpin and F. Bueche, J. Appl. Phys. 35, 3142 (1964).

APPENDIX I

CONSTRUCTION AND OPERATION OF THE VACUUM RELAXOMETER

A relaxometer was designed for studying the thermal stability of crosslinked PMMA polymers at elevated temperatures under vacuum and other environmental conditions by the continuous and intermittent stress-relaxation method. For this purpose, specimens for the continuous and intermittent tests should be subjected to identical vacuum and thermal conditions. This Appendix gives a detailed description of the apparatus constructed and the operational procedures.

A. Description of the Apparatus

1. Mechanical Construction and Layout

The relaxometer, shown in Fig. I-1, is constructed on both sides of a large brass plate supported about five feet above the floor by an angle-iron frame. A circular vacuum plate is mounted about 3 inches below and parallel to the brass plate. Attached beneath the vacuum plate is a 6-inch brass can in which are the load cells, specimens, and the lower portion of the extension rods used to stretch the specimens; the front of the can is cut away, exposing the enclosed components (Fig. I-1). Either an 8-inch glass bell jar or an equivalent copper vessel is placed around the cut-away brass can and mounted flush with the vacuum plate to form a vacuum chamber.

Above the main brass plate are mounted the diffusion pump, cold trap, vacuum gages, bath agitation motor, and a framework which guides the extension rods which extend through the brass and vacuum plates into the vacuum chamber below. Silicone Red Rubber O-rings* are used to form the necessary seals where the extension rods pass through the vacuum plate and also where the copper vessel (or bell jar) meets the vacuum

*Porter Seal Company, Hayward, California.

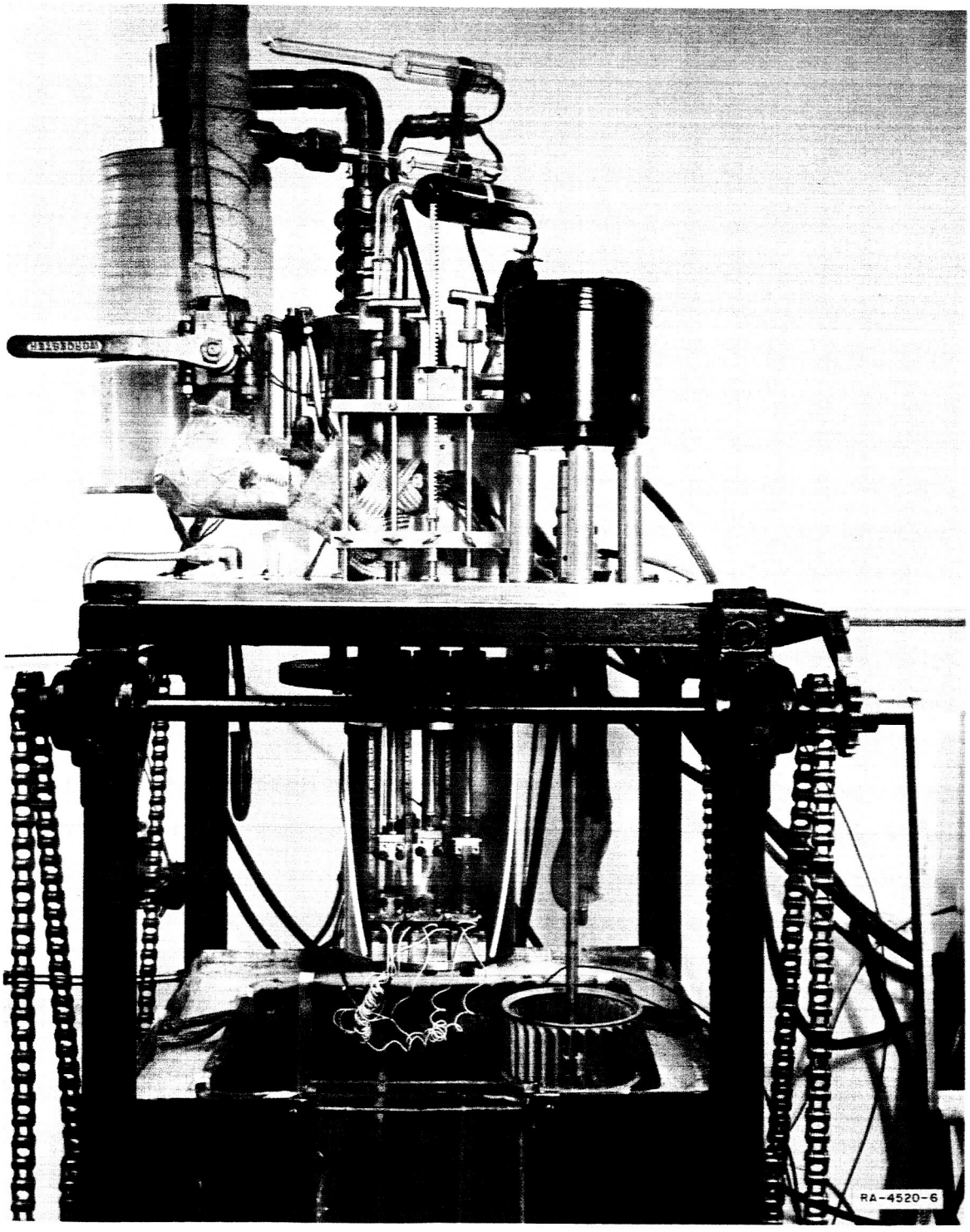

FIG. I-1 PHOTOGRAPH OF VACUUM RELAXOMETER

plate. (Although the O-rings acquired some permanent set at 250°, they were still suitable for two or three successive tests.)

The apparatus contains three load stations. At each station, the clamp at the upper end of a specimen is attached to an extension rod; the lower clamp is attached to a cantilever beam load cell which is mounted on the bottom of the brass can. Figure I-1 shows the clamps used for strip specimens. However, the data presented in this report were obtained on ring-type specimens; such a specimen is placed loosely over specially designed hooks, the upper one being connected to the extension rod with a stainless steel point-contact link to minimize heat conduction. Heat conduction at the lower hook was reduced by mounting the attached load-cells on knife-edges.

The extension rod at the center load station can be raised slowly by a worm gear and rack-and-pinion assembly. This station is used to obtain a preliminary indication of the force which is expected when the other two specimens are extended. Specimens at the left and right load stations are extended rapidly using the handle attached to the upper end of each extension rod. As shown in Fig. I-1, each extension rod is threaded above the brass plate and is fitted with a knurled nut between the main brass plate and a horizontal upper-limit bar. By positioning the nut, the upward travel of an extension rod is limited and a specimen can be quickly extended to the desired amount.

Temperature in the vacuum chamber is maintained by a stirred liquid bath consisting of two concentric metal tanks with insulation in the annular space. The bath, which is suspended on chains, is raised with a crank until the vacuum chamber and vacuum plate are completely immersed in the bath liquid. The bath liquid is a eutectic mixture of 53% potassium nitrate, 7% sodium nitrate, and 40% sodium nitrite. This mixture, which has a melting point of about 140°C, is stable at temperatures up to about 450°C for an indefinite period. The bath is heated by two 500-watt stainless steel immersion heaters. One heater is operated continuously at the power level which yields about 90% of the heat necessary to maintain test temperature; the other heater is activated by a thermal regulator and relay. Nine calibrated copper-constantan thermocouples are

used to measure temperature; six are placed within the vacuum chamber and the remaining three at various points in the bath.

Vacuum is obtained with a Welch Model 5-71740 forepump in series with a CEC Model VFM-10 oil diffusion pump. Pressure is determined with a Pirani gage at pressures down to about one micron and with a hot-cathode ionization gage at lower pressures. The Pirani gage is mounted in the one-inch-diameter copper vacuum line about 20 inches from the vacuum chamber and about the same distance from the diffusion pump. It was not practical to place the gage much closer to the vacuum chamber since the high temperatures would interfere with gage operation.

2. Load Cells and Electrical Components

Because small forces were to be measured, the load cells were placed inside the vacuum chamber to avoid the errors which result from transmitting a force through a sealing ring to an external load cell. Thus, special load cells were constructed to withstand high temperatures. Each load cell consists of a 17-7 PH stainless steel cantilever beam, approximately 2.75 inches long and 0.5 inch wide, fastened horizontally to the bottom of the brass can inside the vacuum chamber. A resistance strain gage* is welded on both the top and bottom surfaces of the beam where the stress in a bent beam is a maximum. The components of the load cell are coated with an inorganic cement which does not evolve gaseous products at elevated temperatures. The beam in a load cell is 0.025 inch thick; forces up to 400 grams can be determined. Flexural oscillations of the thin beam prevent measurements at times shorter than about one second. Load cells which have higher capacity were made using thicker beams, but these were not used for the tests discussed in this report.

The two strain gages in a load cell constitute adjacent arms of a Wheatstone bridge (Fig. I-2) excited by 5-10 volts D.C. Upon applying a force to the load cell, the resistance change in the strain gages causes a voltage imbalance which is proportional to the force. Placement

*Microdot Corporation, Instrumentation Division, 220 Pasadena Ave., South Pasadena, California. Type SG 101-A-1.

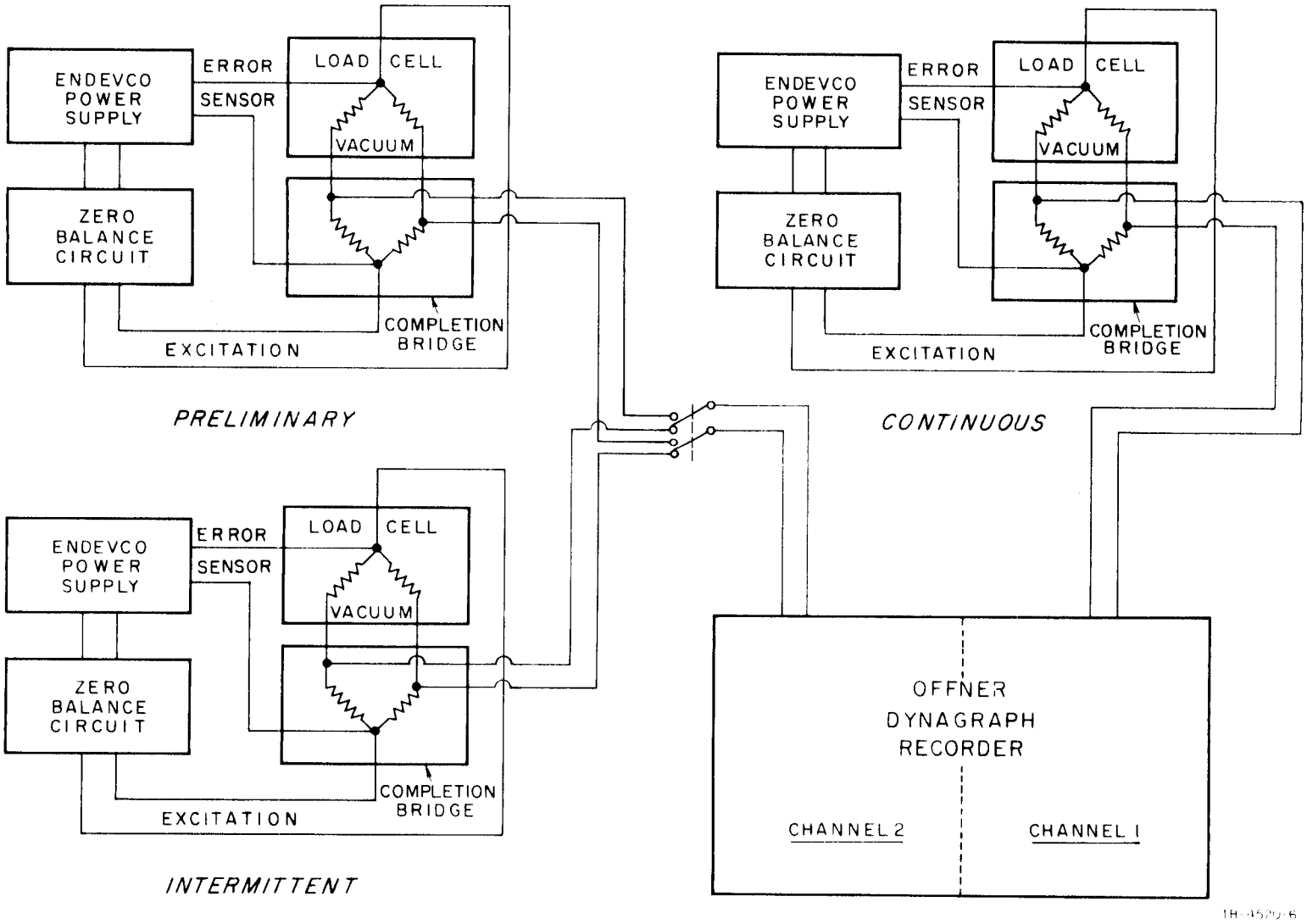

FIG. I-2 BLOCK DIAGRAM OF ELECTRONIC COMPONENTS FOR VACUUM RELAXOMETER

of the strain gages in adjacent arms of the bridge improves the temperature stability, since spurious outputs tend to cancel. The other (completion) arms of the bridge, located outside the apparatus, are matched precision wire-wound Manganin resistors, chosen to minimize bridge imbalances caused by changes in room temperature.

The strain gages are heat treated to obtain a negative change in resistance with temperature which partially compensates for the increase in resistance (and resultant bridge imbalance) caused by thermal expansion of the beam. Tests made at 10 volts excitation at 250°C showed that the residual imbalance was about 1 millivolt. Before each test, this electrical imbalance was zeroed out using a balancing circuit. Although the inherent sensitivity of an individual strain gage decreases by about 0.018%/°C, this change is not reflected in the load cell sensitivity because the flexural modulus of a stainless steel beam also decreases with temperature. For a given force, the increased deflection of the beam at higher temperatures tends to compensate for the decreased sensitivity of the strain gages, and the load cell sensitivity should remain relatively constant.

Separate excitation is provided for each of the three load cells, as shown in Fig. I-2. The power supplies* have their positive error sensor leads connected to the strain gages inside the vacuum chamber; this insures that the excitation voltage on the strain gages remains identical with that developed within the power supply. In this way, a drift in the excitation voltage is eliminated.

An imbalance in the load cell circuit is zeroed out by two variable resistors in parallel with the bridge and with their center taps connected to the positive side of the bridge output. One resistor (10 K Ω) is used for coarse adjustment, while the other (a variable 10 K Ω resistor between two 500 K Ω fixed resistors) is used for fine adjustment.

*Endevco Model SR-200 EHP solid-state feedback type, Endevco Corporation, 801 South Arroyo Parkway, Pasadena, California.

Figure I-2 shows the electrical connections among the strain gages, bridge completion resistors, balancing circuits, and the two-channel recorder.* A switch allows selection of output from either the center ("preliminary") or right load cell.

B. Operational Procedures

Initial tests were made on rectangular strip specimens. However, an accurate adjustment of the bridge imbalance at the test temperature could not be made owing to the thermal expansion of a specimen which produced a force on the load cell. Also, the specimens tended to slip and rupture in the clamps. Thus, the ring-type specimens used for tensile tests (Appendix II) were selected for use in the relaxometer. A ring was placed over hooks (each hook is actually a special device containing a rod to support the ring) attached to the load cell and extension rod in the relaxometer.

Prior to inserting the ring specimens, each of the three load cells was calibrated with a 100-gram weight attached to a hook which was underneath the load cell and extended through the brass can to the load cell. Although this loading deforms a load cell in the direction opposite to that during a relaxation test, calibration tests made by loading the load cells in the opposite direction showed no difference in the electrical output. As part of the calibration procedure, the excitation voltage was adjusted to give an output of 1 millivolt per 100 grams, and the recorder sensitivity was set to give an appropriate displacement on the recorder chart for the expected load.

Each specimen was cleaned with methanol and weighed, and its thickness and diameter were measured. Thoroughly cleaned hooks were attached to the load cells and extension rods, and the specimens were placed loosely over the hooks. After balancing the load cell bridge circuits, each extension rod was slowly raised by turning the knurled nut until a slight deflection on the recorder showed that the specimen was in

*Type R-S two-channel Offner Dynagraph, Beckman Instruments, Inc., Offner Division, 3900 River Road, Schiller Park, Illinois.

contact with the hooks. The copper vacuum housing was then installed and the assembly was evacuated for several hours (usually overnight) at room temperature.

To speed attainment of thermal equilibrium, the liquid bath was heated 20-40°C above the desired test temperature and then raised to surround the vacuum chamber. Adsorption of heat by the chamber brought the bath and specimens to the test temperature nearly simultaneously in about 1.5-2 hours.

After thermal equilibrium had been attained, the position of a scribe mark on each extension rod was measured with a cathetometer, and the residual electrical imbalance in each bridge circuit was zeroed out. The upper limit bar was lowered against the tops of the knurled nuts on the extension rods and it was firmly locked to the center extension rod with a setscrew. The center rod was then raised slowly, extending the specimen and carrying the limit bar upward. When the desired extension was attained (indicated by the position of the scribe mark), the limit bar was locked to the guides by setscrews. This procedure insured that the remaining two specimens could be extended by the same amount as the center specimen.

Continuous measurements were begun on the specimen at the left load station by rapidly pulling the extension rod until the knurled nut hit the upper limit bar; the rod was locked in this position by a setscrew on the limit bar. The developed force was monitored continuously with the recorder while it was changing rapidly; subsequently, it was periodically determined.

Intermittent measurements were begun at the right load station a few minutes following initiation of the continuous test. These were started by extending the specimen rapidly, as in a continuous test, holding it in the extended position for a short time while measuring the force on the recorder, then returning it to its initial unstressed position. This procedure was repeated periodically.

To determine the extent of electrical drift during a test, the load on the continuously stressed specimen was occasionally released for a

short period to observe the recorder baseline. For the intermittently loaded specimen, the baseline was always known before and after each loading.

During the course of a run, the six thermocouples were used to monitor the temperature and its distribution. Two thermocouples, each capped with a small piece of PMMA, were placed near each of the three specimens. These measurements as well as others with the thermocouples in direct contack with various parts of the apparatus showed that the temperature was uniform to within one degree throughout the chamber. Previous tests with thermocouples embedded directly in strip specimens showed the temperature gradient in a specimen was less than one degree. The temperature drift during a run lasting several days was no more than one or two degrees.

The pressure shown by the Pirani gage was always less than 0.1 micron before the chamber was raised to the test temperature. Immediately after immersing the chamber in the bath, the pressure typically increased to 10-15 microns, but it decreased to 3-5 microns during the period required for thermal equilibration of the specimens. The pressure normally decreased further, depending on the temperature and specimen characteristics; a maximum pressure of about one micron ordinarily existed at 250°C, and a pressure of a few tenths of a micron at 180°C.

Tests were made at about a 10% strain, although the actual strain could not be determined conveniently and probably differed appreciably from 10%. The problem in determining the strain results from the sizable thermal expansion of various components in the apparatus and also from the relatively high compliance of the load cell. Because the primary purpose of the work was to obtain relaxation data for which only the change in force is needed (the decay in the relative force is independent of the strain magnitude), a special effort was not made to determine the strain precisely.

APPENDIX II

PROCEDURES FOR OBTAINING TENSILE DATA

Tensile data were obtained by testing rings of the PMMA polymers with an Instron tester which has a temperature-controlled telescoping cabinet.* Specimens were placed in the cabinet precisely 10 minutes before being tested, a period sufficient for thermal equilibration but not long enough for chemical degradation to occur.

Ring specimens were prepared from sheets of the PMMA polymers by first cutting discs having a diameter slightly greater than 1.5 inches, the desired outside diameter for a specimen. Several discs were stacked and then turned on a lathe to a diameter of 1.5 inches; this outside diameter was measured precisely with a vernier caliper. These finished discs were then placed (two or three at a time) in a special socket mounted on the lathe and bored to an inside diameter of about 1.35 inches.

The thickness of each ring was obtained by an indirect method. Each of twenty or more rings having the same outside and inside diameters was cleaned and weighed on an analytical balance. The thickness of each ring was measured at three points with a dial gauge to obtain an average thickness. These data were used to compute a linear regression line (thickness on weight) having a slope

$$b = \sum_i w_i t_i / \sum_i w_i^2$$

where w_i is the weight of an individual ring, and t_i is its average thickness. After b was obtained, the thickness of each ring was calculated from $t_i = bW_i$.

The inside diameter of each ring was calculated from the outside diameter, thickness, and weight of the ring, and the density of the material (determined by the buoyancy method) according to $D_i^2 = D_o^2 - 0.0777\ W/\rho t$, where D_i and D_o are, respectively, the inside and outside

*See Ref. 7 on page 64 of this report.

diameters in inches, W and t are the weight in grams and thickness in inches, and ρ is the density in g/cm^3.

In deriving values of stress and strain from an Instron trace (a plot of force against time), the dimensions of a ring at the test temperature were used. The dimensions were calculated from the dimensions at room temperature and the coefficients of thermal expansion for PMMA below and above the glass temperature (S. Loschaek, J. Polymer Sci. 15, 391 (1955). The strain, $\lambda-1$, was calculated from the crosshead displacement, ΔL, using the equation:*

$$\lambda-1 = \frac{4\Delta L}{\pi(D_o+D_i)} - \frac{(D_o-D_i)}{(D_o+D_i)}\left[1 - \lambda^{-\frac{1}{2}}\right] \qquad \text{(III-1)}$$

This equation* gives the average strain in the ring. The stress was obtained from the force and the cross-sectional area of the unstressed specimen; for a ring specimen this area equals $(D_o-D_i)t$.

Rupture strains were based on the inside diameter of a ring and were computed from the equation:

$$\lambda_b-1 = \frac{2\Delta L}{\pi D_i} \qquad \text{(III-2)}$$

Values of the rupture stress were obtained by extrapolating a force-time trace beyond rupture up to the point at which the average strain in the ring equals that based on the inside diameter. A discussion of the validity of this procedure is given elsewhere.*

To reduce a force-time trace, a large number of points were read from the trace with an Oscar read-out device attached to a key punch for recording the data on punch cards. The quantities required to prepare the plots of log σ vs. log t, as well as certain other plots, were computed on a Burroughs B-5500 Computer.

*See Ref. 7 on page 64 of this report. The equation on page 142 of the referenced publication contains an erroneous factor of 2 in the second term on the right side of the equation.

APPENDIX III

LITERATURE SURVEY*

During the initial quarter of this project, a survey was made of literature on mechanical and stability characteristics of PMMA and PMMA-EDMA copolymers. The information presently in Quarterly Technical Summary Report No. 1 is reproduced below.

A. Viscoelastic Properties of PMMA

PMMA is one of the most extensively studied amorphous polymers. Its viscoelastic properties have been investigated by stress relaxation* (5, 14, 16, 22, 26, 39, 67), creep (16, 26, 34, 47, 67), and dynamical methods (1, 3, 16, 27, 42). Mechanical damping data have also been obtained by a number of workers (9, 15, 16, 20, 21, 24, 28, 29, 32, 33, 49, 50, 55, 56, 61, 66), and the results summarized by Woodward and Sauer (65). These extensive studies have clearly established the existence of at least two transition regions in the mechanical properties of PMMA. The regions show up as peaks or as changes in levels of the viscoelastic functions. By comparing the results from mechanical, dielectrical, and nuclear magnetic resonance measurements (46, 48, 65), it has been possible to assign the main or α-transition to the excitation of main chain motion, and the secondary or β-transition to excitation of side chain motion. The activation energy for the β-process, about 20 kcal/mole (9), is much smaller than that for the α-process, which is of the order of 100 kcal/mole (20).

The behavior of PMMA in creep at large stresses below the glass temperature was investigated by Wall (62), Marin and co-workers (40,41), and Sherby and Dorn (52).

B. Transition Temperatures of PMMA

The temperature at which chain motions are frozen is shown by a change in the first derivatives (coefficient of expansion, specific heat, etc.) of the primary thermodynamic properties (volume, energy, etc.). From the theoretical viewpoint, the concept of a transition

*The reference list begins on page 82 and the references there are coded A-1, A-2, etc. to distinguish them from those referenced in other sections of this report.

temperature as a material constant is a difficult one (46). Furthermore, it is clear from the discussion by Ferry (11), and by Saito et al. (46) that determined transition temperatures depend on the thermal path, and the data are to some extent arbitrary even when obtained on an ideal sample which is free from impurities and is homogeneous with respect to molecular weight and chain structure. Nevertheless, if the theoretical and experimental limitations are kept in mind, the transition temperature concept assists materially in explaining polymer behavior.

The occurrence of a transition temperature corresponding to the β-transition in PMMA has not been conclusively demonstrated, although it has been claimed to occur around 0° to 5°C (9, 53). The temperature related to the α-transition, or glass temperature T_g, has been found to be 105°C by Fox and Loshaek (13), and by Rogers and Mandelkern (45). Fujino, Senshu, and Kawai (14) pointed out that the break in Rogers and Mandelkern's plot of specific volume against temperature seems to occur at 100° rather than at 105°C and they used this value in their calculations. The volume-temperature plot shown by Saito et al. (46) and apparently obtained by Hideshima (46a), displays a single break near 96°C. Rogers and Mandelkern's data may be reinterpreted to give a similar value for T_g. It must be noted that, apart from the thermal path chosen, the glass temperature is affected not only by differences in molecular weight distribution and the presence of spurious impurities and residual plasticizing components such as MMA, but also by the stereoregularity of the sample which depends on the conditions under which polymerization is carried out. The syndiotactic chain is stiffer than the isotactic; its glass temperature is 115°C while that of isotactic PMMA is 45°C (12, 17, 30, 43, 44, 54). Conventional PMMA is probably predominantly syndiotactic.

Evidently T_g as customarily determined will be a characteristic of an individual sample under identical experimental conditions. For PMMA, 100°C seems to be a reasonable average value. For PMMA crosslinked with GDMA, Loshaek (36) found that T_g increases with the degree of crosslinking.

The concept of the glass transition in polymers is usually linked with the concept of free volume (11). According to this view, a lowering of the temperature is accompanied by a collapse of free volume. Above T_g the volume contraction is of a liquidlike character. Below T_g the free volume remains more nearly constant, and exhibits an essentially solidlike behavior. Considerations of changes in free volume predict a dependence of the viscoelastic properties of polymers on their thermal history. The influence of cooling rate on the stress relaxation of PMMA at temperatures below T_g has been demonstrated by McLoughlin and Tobolsky (38, 39), but no systematic investigation of this effect, particularly on the failure properties of PMMA, has been reported.

C. Ultimate Tensile Properties of PMMA

Valuable information on the ultimate (failure) tensile properties of polymers may be obtained from stress-strain curves (often obtained at constant rates of strain) determined to the point of failure. Such curves on PMMA have been reported in several studies (10, 31, 67) but are not particularly suited for developing a comprehensive picture of the failure behavior.

Failure at high temperatures or low rates of strain is referred to as tough failure and is usually accompanied by necking (57) or cold-drawing (57) of the specimen, resulting in large elongations-at-break, and a distinctive appearance of the failure surface. Stress-strain curves obtained under conditions leading to tough failure often show a yield point and a plateau region corresponding to necking or cold-drawing when the stress is calculated on the initial cross section of the specimen. The stress at the yield point is known as the yield strength and the corresponding extension as the yield elongation.

Brittle failure occurs at low temperatures or high rates of strain. It is characterized by a monotonic stress-strain curve, small elongation-at-break, the absence of necking or cold-drawing, and a different morphology of the failure surface. The temperature transition between

brittle and tough failure is known as the brittle point. Brittle strength is the stress-at-break in brittle failure. The area under the stress-strain curve is called the fracture energy, or energy-to-break.

The tough and brittle failure of PMMA has been studied extensively (4, 23, 51, 58-60). Hoff(23) investigated the recovery of deformation beyond the yield point and showed that there is very little permanent set (plastic deformation) in PMMA, the deformation being generally recoverable by heat treatment (52). The morphology of the failure surface of PMMA has been discussed by various authors (6, 51, 63). Coulehan (7) and Wolock et al., (64) discussed the stress-crazing of PMMA, a phenomenon that may lead to catastrophic failure of the sample when brought into contact with certain liquids.

D. Thermal Degradation and Self-plasticization of PMMA

The thermal degradation of PMMA has been studied by Grassie and Melville (18), Cowley and Melville (8), and Lohr and Parker (35). The main degradation product is the monomer, MMA. A degraded sample will therefore contain the monomer as a plasticizing component. The presence of a plasticizing component strongly influences the mechanical behavior of polymers. McLoughlin and Tobolsky (39) have shown the effect of water as a plasticizer in PMMA. The influence of monomer content (self-plasticization) on the glass temperature of PMMA was investigated by Aleksandrov and Lazurkin (2), while Lohr and Parker (35) studied the effect of monomer content on the tensile yield strength of PMMA.

E. Crosslinked PMMA (PMMA-EDMA Copolymers)

The literature contains relatively little information on PMMA-EDMA copolymers which is relevant to the present study. Loshaek (13, 36, 37) showed that the glass temperature increases with the degree of crosslinking. Grassie and Melville (19) studied the thermal degradation of PMMA-EDMA copolymers. As with uncrosslinked PMMA, the main degradation product is MMA and the degree of crosslinking had no effect on the degradation. It was concluded that

when a chain degradation reaches a junction point in the network, the unit containing it will be eliminated in the normal way, i.e., as with uncrosslinked PMMA. The EDMA molecule will not, however, be evolved until both chains of which it has been a part, have been depolymerized.

Heijboer (20, 21) reported the influence of crosslinking on the mechanical damping, and some stress-strain curves were obtained by Knowles and Dietz(31). Vincent (58) remarked that the effect of crosslinking generally is to increase the modulus and the yield strength in the tough region at a given temperature but that crosslinking (up to 5% EDMA) has little effect on the brittle strength.

BIBLIOGRAPHY

A- 1. A. P. Aleksandrov and J. S. Lazurkin, "Polymers I., Highly Elastic Deformation in Polymers," Acta Physicochim. URSS 12; 647-668 (1940).

A- 2. A. P. Aleksandrov and J. S. Lazurkin, "Softening Temperature of Polymers," Compt. Rend. Acad. Sci. URSS 43:276-379 (1944).

A- 3. G. W. Becker, "Mechanische Relaxationserscheinungen in nicht weichgemachten hochpolymeren Kunststoffen," Kolloid-Z. 140; 1-32 (1955).

A- 4. J. P. Berry, "Fracture Processes in Polymeric Materials. I., The Surface Energy of Poly(methyl Methacrylate)," J. Polymer Sci. 50; 107-115 (1961).

A- 5. J. Bischoff, E. Catsiff, and A. V. Tobolsky, "Elastoviscous Properties of Amorphous Polymers in the Transition Region. I.," J. Amer. Chem. Soc. 74:3378-3381 (1952).

A- 6. W. F. Busse, E. Orowan, and J. E. Neimark, "Morphology of Fractures in Polymethyl Methacrylate." Paper presented before the Am. Phys. Soc., Philadelphia, Pa., March 1957.

A- 7. R. E. Coulehan, "The Rheology of Stress Crazing," Paper presented before the Fourth International Congress on Rheology, Providence, R. I., August 1963.

A- 8. P. R. E. J. Cowley and H. W. Melville, "The Photo-degradation of Polymethylmethacrylate," Proc.Roy.Soc.A210:461-481 (1952); A211:320-334 (1952).

A- 9. K. Deutsch, E. A. W. Hoff, and W. Reddish, "Relation Between the Structure of Polymers and Their Dynamic Mechanical and Electrical Properties. Part I. Some Alpha-substituted Acrylic Ester Polymers," J. Polymer Sci. 13:565-582 (1954).

A-10. A. G. H. Dietz, W. J. Gailus, and S. Yurenka, "Effect of Speed of Test Upon Strength Properties of Plastics," ASTM Proc. 48; 1160-1186 (1948).

A-11. J. D. Ferry, "Viscoelastic Properties of Polymers," Wiley, New York, 1961.

A-12. T. G. Fox, B. S. Garrett, W. E. Goode, S. Gratch, J. F. Kincaid, A. Spell, and J. D. Stroupe, "Crystalline Polymers of Methyl Methacrylates," J. Am. Chem. Soc. 80:1768-1769 (1958).

A-13. T. G. Fox and S. Loshaek, "Influence of Molecular Weight and Degree of Cross-linking on the Specific Volume and Glass Temperature of Polymers," J. Polymer Sci. 15:371-390 (1955).

A-14. K. Fujino, K. Senshu, and H. Kawai, "Tensile Stress Relaxation Behavior of Methylmethacrylate and Methylacrylate Copolymers," J. Colloid Sci. 16:262-283 (1961).

A-15. E. Fukada, "On the Relation between Creep and Vibrational Loss of Polymethylmethacrylate," J. Phys. Soc. Japan 6:254-256 (1951).

A-16. E. Fukada, "The Relation Between Dynamic Elastic Modulus, Internal Friction, Creep and Stress Relaxation in Polymethylmethacrylate," J. Phys. Soc. Japan 9:786-789 (1954).

A-17. W. G. Gall and N. G. McCrum, "Internal Friction in Stereoregular Polymethyl Methacrylate," J. Polymer Sci. 50:489-495 (1961).

A-18. N. Grassie and H. W. Melville, "The Thermal Degradation of Polyvinyl Compounds," Proc. Roy. Soc. A199:1-13, 14-23, 24-39 (1949).

A-19. N. Grassie and H. W. Melville, "The Thermal Degradation of Polyvinyl Compounds, IV. The Thermal Degradation of the Methyl Methacrylate Copolymers with Glycol Dimethacrylate and Acrylonitrile," Proc. Roy. Soc. A199:39-55 (1949).

A-20. J. Heijboer, "Molekulare Deutung Sekundarer Dampfungsmaxima. Bewegungen von Atomgruppen in Polymethacrylaten im Glasszustand." Kolloid-Z 148:36-46 (1956).

A-21. J. Heijboer, P. Dekking and A. J. Staverman, "The Secondary Maximum in the Mechanical Damping of Polymethyl Methacrylate: Influence of Temperature and Chemical Modification," Proc. 2nd Int'l Congr. Rheology, Butterworths, London, 1957, pp. 123-132.

A-22. T. Hideshima, H. Nakane, and S. Iwayanagi, "Stress Relaxation and Relaxation Spectrum of Polymethyl Methacrylate in its Secondary Dispersion Region." Paper presented before the 7th Canadian High Polymer Forum, Sarnia, 1956.

A-23. E. A. W. Hoff, "Some Mechanical Properties of a Commercial Polymethylmethacrylate," J. Appl. Chem. 2:441-448 (1952).

A-24. E. A. W. Hoff, D. W. Robinson, and A. H. Willbourn, "Relation Between the Structure of Polymers and their Dynamic Mechanical and Electrical Properties. Part II. Glassy State Mechanical Dispersions in Acrylic Polymers," J. Polymer Sci. 18:161-176 (1955).

A-25. D. S. Hughes, E. B. Blankenship, and R. L. Mims, "Variation of Elastic Moduli and Wave Velocity with Pressure and Temperature in Plastics," J. Appl. Phys. 21:294-297 (1950).

A-26. S. Iwayanagi, "On the Viscoelastic Properties of Polymethylmethacrylate," J. Sci. Research Inst. (Japan) 49:4-12 (1955).

A-27. S. Iwayanagi and T. Hideshima, "Dynamical Study on the Secondary Anomalous Absorption Region of Polymethylmethacrylate," J. Phys. Soc. Japan 8:368-371 (1953).

A-28. E. Jenckel, "Zur Schwingungsdampfung in Hochpolymeren," Kolloid-Z 136:142-152 (1954).

A-29. E. Jenckel and K. H. Illers, "Uber die Temperaturabhangigkeit der inneren Dampfung von weichgemachtem Polymethacrylsauremethylester," Z. Naturforsch 99:440-450 (1954).

A-30. V. A. Kargin, V. A. Kabanov, and V. P. Zubov, "The Production of Isotactic Polymethylmethacrylate by Polymerization of the Frozen Monomer," Polymer Sci. USSR 2:261-263 (1961); Vysokomol. Soedin. 2:303-305 (1960).

A-31. J. K. Knowles and A. G. H. Dietz, "Viscoelasticity of Polymethyl Methacrylate - An Experimental and Analytical Study," Trans. ASME, 77:177-186 (1955).

A-32. J. Koppelmann, "Uber die Bestimmung des dynamischen Elastizitatsmoduls und des dynamischen Schubmoduls im Frequenzbereich von 10^{-5} bis 10^{-1} Hz," Rheol. Acta 1:20-28 (1958).

A-33. J. Koppelmann, "Uber den dynamischen Elastizitatsmodul von Polymethacrylsauremethylester bei sehr tiefen Temperaturen," Kolloid-Z 164:31-34 (1959).

A-34. W. Lethersich, "The Rheological Properties of Dielectric Polymers," Brit. J. Appl. Phys. 1:294-301 (1950).

A-35. J. J. Lohr and J. A. Parker, "The Combined Effects of Ultraviolet Radiation and Vacuum on the Tensile Yield Properties of Polymethylmethacrylate," Paper presented before the Division of Polymer Chemistry, at the Fall Meeting of the American Chemical Society, New York City, 1963. ACS Polymer Preprints 4:363-377 (1963).

A-36. S. Loshaek, "Crosslinked Polymers. II. Glass Temperatures of Copolymers of Methyl Methacrylates and Glycol Dimethacrylates," J. Polymer Sci. 15:391-404 (1955).

A-37. S. Loshaek and T. G. Fox, "Cross-linked Polymers. I. Factors Influencing the Efficiency of Cross-linking in Copolymers of Methyl Methacrylate and Glycol Dimethacrylates," J. Am. Chem. Soc. 75:3544-3550 (1953).

A-38. J. R. McLoughlin and A. V. Tobolsky, "Effect of Cooling Rate on Stress Relaxation of Polymethylmethacrylate," J. Polymer Sci. 7:658 (1951).

A-39. J. R. McLoughlin and A. V. Tobolsky, "The Viscoelastic Behavior of Polymethylmethacrylate," J. Colloid Sci. 7:555-568 (1952).

A-40. J. Marin and Y. Pao, "On the Accuracy of Extrapolated Creep-Test Relations for Plexiglas Subjected to Various Stresses," Trans. ASME 74:1231-1240 (1952).

A-41. J. Marin, Y. Pao, and G. Cuff, "Creep Properties of Lucite and Plexiglas for Tension, Compression, Bending, and Torsion," Trans. ASME 73:705-719 (1951).

A-42. B. Maxwell, "An Investigation of the Dynamic Mechanical Properties of Polymethylmethacrylate," J. Polymer Sci. 20; 551-563 (1956).

A-43. R. G. J. Miller, B. Mills, P. A. Small, A. Turner-Jones, and D. G. M. Wood, "Crystalline Poly (Methyl Methacrylate)," Chem. and Ind. 1323-1324 (1958).

A-44. A. Odajima, A. E. Woodward, and J. A. Sauer, "Proton Magnetic Resonance of Some α-Methyl Group Containing Polymers and Their Monomers," J. Polymer Sci. 55:181-196 (1961).

A-45. S. S. Rogers and L. Mandelkern, "Glass Formation of Polymers. I. The Glass Transitions of the Poly-(n-Alkyl Methacrylates), J. Phys. Chem. 61:985-990 (1957).

A-46. N. Saito, K. Okano, S. Iwayanagi, and T. Hideshima, "Molecular Motion in Solid State Polymers," Solid State Physics, Vol. 14, Academic Press, New York, 1963. (a) See p. 494, and references 293 and 295.

A-47. K. Sato, H. Nakane, T. Hideshima, and S. Iwayanagi, "Creep of Polymethyl Methacrylate at Low Temperature," J. Phys. Soc. Japan 9:413-416 (1954).

A-48. J. A. Sauer and A. E. Woodward, "Transitions in Polymers by Nuclear Magnetic Resonance and Dynamic Mechanical Methods," Rev. Modern Phys. 32:88-101 (1960).

A-49. K. Schmieder and K. Wolf, "Uber die Temperatur-und Frequenzabhangigkeit des mechanischen Verhaltens einiger hochpolymeren Stoffe," Kolloid-Z. 127:65-78 (1952).

A-50. K. Schmieder and K. Wolf, "Mechanische Relaxationserscheinungen an Hochpolymeren (Beziehungen zur Struktur)," Kolloid-Z. 134; 149-184 (1953).

A-51. F. Schwarzl and A.J. Staverman, "Bruchspannung und Festigkeit von Hochpolymeren," in: H.A. Stuart: "Die Physik der Hochpolymeren," Vol. IV, Springer, Gottingen, 1956.

A-52. O.D. Sherby and J.E. Dorn, "Anelastic Creep of Polymethylmethacrylate," J. Mech. and Phys. Solids 6:145-162 (1958).

A-53. M.C. Slone, J.J. Lamb, and F.W. Rinehart, "Properties of Polymethyl Alpha-chloroacrylate," Modern Plastics, June 1952, p. 109.

A-54. J.D. Stroupe and R.E. Hughes, "The Structure of Crystalline Poly-(Methyl Methacrylate)," J. Am. Chem. Soc. 80:2341-2342 (1958).

A-55. H. Thurn and K. Wolf, "Dielektrizitatskonstante und mechanische Verluste bei Hochpolymeren," Z. angew. Phys. 7:44-47 (1955).

A-56. H. Thurn and K. Wolf, "Vergleichende dielektrische und Ultra-schallmessungen bei 2.10^6 Hz an Polyvinylestern, Polyacrylestern, und Polyvinylathern," Kolloid-Z.148:16-50 (1956).

A-57. P.I. Vincent, "The Necking and Cold-drawing of Rigid Plastics," Polymer 1:7-19 (1960).

A-58. P.I. Vincent, "The Tough-Brittle Transition in Thermoplastics," Polymer 1:425-444 (1960).

A-59. P.I. Vincent, "The Rupture Factor of Polymethylmethacrylate," British J. Appl. Physics 13:578-582 (1962).

A-60. P.I. Vincent, "Strength of Plastics," Part 1-9, Plastics (London), Oct., Nov. (1961), Jan., Feb. (1962), April-July (1962), August (1962).

A-61. Y. Wada and K. Yamamoto, "Temperature Dependence of Velocity and Attenuation of Ultrasonic Waves in High Polymers," J. Phys. Soc. Japan 11:887-892 (1956).

A-62. W.C. Wall, "Design Information on Lucite," Aero Digest 41; 122, 124, 126, 128-9, 254 (1942).

A-63. I. Wolock, J.A. Kies, and S.B. Newman, "Fracture Phenomena in Polymers," in: B.L. Averbach et al: "Fracture," Wiley, New York, 1959.

A-64. I. Wolock, M.A. Sherman, and B.M. Axilrod, "Effects of Molecular Weight on Crazing and Tensile Properties of Polymethyl Methacrylate," NACA Research Memorandum 54A04 (1954).

A-65. A.E. Woodward and J.A. Sauer, "The Dynamic Mechanical Properties of High Polymers at Low Temperatures," Fortschr. Hochpolym. - Forsch. 1:114-158 (1958).

A-66. K. Yamamoto and Y. Wada, "Investigation of Dynamic Mechanical Properties of Glassy Polymers by Composite Oscillator Method," J. Phys. Soc. Japan 12:374-378 (1957).

A-67. S. Yurenka, "Creep and Relaxation Properties of Polymethylmethacrylate," Thesis, MIT, Dept. Mech. Eng., Cambridge, Mass., 1950.